

Study of High Energy Magnetic Bremsstrahlung  
in Pulsed Megagauss Fields

Proposal Submitted  
to  
National Accelerator Laboratory

January 1973

T. Erber  
Department of Physics, Illinois Institute of Technology

C. S. Shen  
Department of Physics, Purdue

RECEIVED

JAN 26 1973

NAL Directors Office

## 1. Project Summary

We propose to perform an experiment at the National Accelerator Laboratory to study the scattering of electrons in the energy range 150 - 300 GeV by pulsed magnetic fields with intensities 1.5 - 3 MG (megagauss). The magnetic Bremsstrahlung (synchrotron radiation) intensities associated with this scattering process are seven orders of magnitude larger than in any previous experiment not utilizing megagauss targets. Under these conditions it will be possible to establish for the first time the existence of the following effects:

- (i) Radiation reaction shifts of the electron trajectories. In the present experiment these correspond to angular deflections given by the Shen-Latal formula [1,2]\*

$$\delta\theta_{CD}(\text{mrad}) = 1.90 \times 10^{-4} H^3(\text{MG})L^2(\text{mm}), \quad (1)$$

where L is the path length in the magnetic field H.

- (ii) Energy straggling induced by quantum effects. This gives rise to an angular spread of the scattered electrons given by the Shen-White formula [3,4]

$$\Delta\theta(\text{mrad}) = \frac{0.95 \times 10^{-3} H^{5/2}(\text{MG})L^{3/2}(\text{mm})}{1 + 1.33 \times 10^{-5} H^2(\text{MG})L(\text{mm}) E_{inc}(\text{GeV})}, \quad (2)$$

where  $E_{inc}$  denotes the incident electron energy at the MG-targets.

- (iii) Radiation reaction and quantum modification of the Bremsstrahlung spectrum and total radiation rate. The

---

\* Bracketed numbers indicate papers cited in the Bibliography at the end of Section 8(a); p. 63.

classical relativistic expression for the total energy radiated into the spectral interval between  $\hbar\omega_1$  and  $\hbar\omega_2$  is

$$\begin{aligned} \mathcal{E}^C(E, H, L, \hbar\omega_1, \hbar\omega_2) &= \\ &= 0.12 H(\text{MG}) L(\text{mm}) \int_{\hbar\omega_1}^{\hbar\omega_2} d(\hbar\omega) \chi \left[ \frac{15 \hbar\omega (\text{MeV})}{H(\text{MG}) E^2 (\text{GeV})} \right] \end{aligned} \quad (3)$$

where  $E$  is the incident electron energy, and

$$\chi(z) = z \int_z^\infty dx K_{5/3}(x).$$

The corresponding quantum mechanical result is

$$\begin{aligned} \mathcal{E}^{QM}(E, H, L, \hbar\omega_1, \hbar\omega_2) &= \\ &0.12 H(\text{MG}) L(\text{mm}) \int_{\hbar\omega_1}^{\hbar\omega_2} d(\hbar\omega) \left[ 1 - \frac{\hbar\omega}{E} \right] \chi \left[ \frac{15 \hbar\omega (\text{MeV})}{H(\text{MG}) E^2 (\text{GeV})} \left\{ 1 + \frac{\hbar\omega}{E} \right\} \right]. \end{aligned} \quad (4)$$

For  $E \sim 300$  GeV,  $H \sim 2$  MG, the discrepancy between (3) and (4) in the spectral range  $\hbar\omega \gtrsim 10$  GeV is 30%.

The proportional difference between the quantum and classical total radiation rates is given by

$$\frac{I^C - I^{QM}}{I^C} \approx 2.63 \times 10^{-4} E(\text{GeV}) H(\text{MG}). \quad (5)$$

For  $E \sim 300$  GeV,  $H \sim 2$  MG, this amounts to a 16% effect.

The technical feasibility of combining megagauss generators with a high energy accelerator has already been demonstrated by an IIT-SLAC collaboration: Megagauss Bremsstrahlung experiments utilizing 19 GeV electron bursts incident on coil and implosion

targets (1 - 1.6 MG) were carried out at SLAC during the period June - November 1970. Complete analyses of these experiments are given in references [5,6,7]. The observed Bremsstrahlung spectra, polarization, and electron deflections agree with the predictions of classical electrodynamics to within 10% --- the nominal accuracy of the experiments. The proposed second series of experiments at NAL should lead to precise measurements of the effects (1) - (5) because of the following factors:

- (A) The essential "signal-to-noise" ratio associated with the detection of the radiation reaction shift (1) is given by

$$\frac{\delta\theta_{CD}}{\theta_0} = 6.33 \times 10^{-6} H^2(\text{MG}) L(\text{mm}) E(\text{GeV}), \quad (6)$$

where  $\theta_0$  is the ordinary Lorentz deflection. We anticipate the following changes in these parameters:

	SLAC	NAL
H(MG)	1.5	2 ( $\rightarrow$ 3)
L(mm)	5	10
E(GeV)	19	300

The ratio (6) therefore is increased by a factor of 50; in fact  $\frac{\delta\theta_{CD}}{\theta_0}(\text{NAL}) \gtrsim 7\%$ . Analogous calculations show that the other effects (2) - (5) are also enhanced well beyond their thresholds of detectability.

- (B) The analytical results (1) - (5) are currently being adapted to the simulation of the effects in the actual experimental set ups by the development of computer codes. These codes are constructed to take into account the primary effects

as well as perturbations due to beam spread, beam divergence, energy variations, target distentions, magnetic field inhomogeneities --- particularly gradient effects at the boundaries of the MG-targets, induced electric fields, and multiple scattering corrections. Theoretical upper bounds for a variety of subsidiary effects, e.g. "Stern-Gerlach" diffraction associated with the electron moment, have been obtained. This thorough preparation for data interpretation and reduction will improve the calibration procedures and increase the precision of the experimental results.

(C) A number of technical improvements are planned for the NAL runs:

- (1) After the conclusion of the SLAC series, it was discovered that MG targets fabricated from tantalum did not distort during the  $2 \mu\text{sec}$  duration of the experiments. This stability is helpful in reducing uncertainties in the determination of the path integral  $\int H d\ell$ . The MG targets for NAL will be redesigned for optimum dimensional stability and reshaped to reduce fringing fields, and to match the field volumes to the beam trajectories.
- (2) The main capacitor bank will be slightly enlarged ( $60 \text{ kJ} \rightarrow 80 \text{ kJ}$ ), and speeded up, e.g. the quarter period reduced from  $2.0 \mu\text{sec}$  to  $1.7 \mu\text{sec}$ . The overall system jitter will also be reduced from  $50 \text{ nsec}$  to  $\sim 10 \text{ nsec}$  by changing the dielectric switch from exploding wire to exploding foil configuration [8], and actuating the discharge with commercial pulse amplifiers.

- (3) We hope to secure approval from NAL to have one member of our group (Dr. D. White) collaborate on a full-time basis on the final design and set-up of the electron/photon beam so that modifications required for the megagauss Bremsstrahlung experiment can be incorporated from the beginning, and that compatibility with other experiments sharing the beam is assured. The following table summarizes the essential parameters of the SLAC D-9 beam which was set up for the initial run of this experiment, the nominal values of the NAL A beam, and the A beam modifications required for a precise measurement of the Bremsstrahlung effects (1) - (5).
- (4) All of the interesting effects (1) - (5) are diminished by factors of the order of  $\left(\frac{m_e}{m_{\mu, \pi}}\right)^4$  for muons and pions. "Contamination" of the NAL A-beam with synchronized bursts of heavier particles will therefore permit an independent check of their experimental detection. We hope to secure approval for incorporating this option in the final design of the A-beam.

The basic reasons for continuing this research program are the following:

- (1) It will lead to a test of the Lorentz-Dirac equation under conditions where perturbation theory cannot be applied [11,12].
- (2) One can study quantum electrodynamics in a regime of strong coupling without strong interactions [13].

Table 1. Summary of Beam Parameters

Properties at Experiment	SLAC D-9 [9]	NAL A-beam [10]	NAL A-beam modified for megagauss Bremsstrahlung Experiment
E (GeV)	19	20 - 300	150 - 300
Momentum resolution (%)	$\pm 0.3$	$\lesssim 2$	$\pm 0.3$
$e^-$ per pulse	$\sim 2 \times 10^6$	$10^7 - 10^8$	$\begin{cases} 10^2 - 10^4 & \text{phase I} \\ 10^4 - 10^7 & \text{phase II} \end{cases}$
Pulse length ( $\mu$ sec)	$\sim 0.3$ (gun program)	20 (fast extraction)	$\lesssim 0.1$ (pulsed magnet)
Horizontal divergence (mrad)	0.3	0.3	$\begin{cases} 0.03 & \text{phase I} \\ 0.3 & \text{phase II} \end{cases}$
Vertical divergence (mrad)	0.3	0.3	0.3
Horizontal beam size (mm)	1.3	13.2	$\begin{cases} \lesssim 1 & \text{phase I} \\ \lesssim 2 & \text{phase II} \end{cases}$
Vertical beam size (mm)	1.3	8.2	$\lesssim 1.5$

Note: Phase I - Measurement of radiation reaction (1) and quantum straggling (2).

Phase II - Measurement of Bremsstrahlung (3) - (5).

- (3) The experimental arrangements planned for NAL will permit the terrestrial simulation of a wide variety of conditions which are of astrophysical interest, particularly magnetic effects associated with some white dwarfs,  $H \sim 10^6 - 10^7$  G [14]; and pulsars,  $H \sim 10^6 - 10^{14}$  G [15,16].

We propose that the megagauss research program at NAL be carried out in several stages:

Phase I. Set up of the modified A-beam and check out of its space-time synchronization properties (Table 1). Set up of capacitor bank and coil equipment capable of generating fields between 2 and 3 MG over path lengths of 10 mm. Measurement of the radiation reaction (1) and energy straggling (2) effects with emulsion techniques.

Phase II: Measurement of the Bremsstrahlung characteristics (4), (5) with counters.

Phase III: Measurement of magnetic Compton scattering ( $\gamma + e + H \rightarrow \gamma + e + H$ ) by modifying the A beam to deliver synchronized  $\gamma$ -bursts ( $E_\gamma \gtrsim 100$  GeV) and fitting MG-targets with exploding wire elements.

Phase IV: Increase field intensities to 4 - 9 MG range by switching to flux compressions driven by helical generators [17,18]. Remeasure effects (1) - (5). Change to a beam configuration capable of delivering 500 GeV  $\gamma$ -rays and look for direct magnetic pair production ( $\gamma + H \rightarrow e^+ + e^- + H$ ) [19].



2. Table of Contents

	<u>Page</u>
1. Project Summary. . . . .	1
2. Table of Contents. . . . .	8
3. Research Personnel . . . . .	10
4. Magnetic Bremsstrahlung. . . . .	16
(a) Radiation Reaction Effects [Uniform Fields]	
(b) Radiation Reaction Effects [Non-Uniform Fields]	
(c) Quantum Fluctuation Effects	
(d) Compton Scattering and Soft Photon Emission	
5. Experimental Design Considerations . . . . .	41
(a) First Things First	
(b) Requirements for Phase I	
(c) Beam Intensity and Emulsion Detectors	
6. Plan of the Complete Experiment. . . . .	53
(a) Condenser Bank	
(b) MG-Target Design	
(c) Instrumentation	
(d) Emulsion Goniometer	
7. The Bremsstrahlung Experiment at NAL . . . . .	59
(a) Listing of Experimental Modules	
(b) Construction of Modified A-Beam	
(c) Beam Time Requirements	
8. (a) References. . . . .	63
(b) Figures . . . . .	65

	Page
9. (a) Budget - IIT Portion. . . . .	74
(b) Budget - Purdue Portion . . . . .	76
(c) Total Budget. . . . .	77
10. Sponsorship. . . . .	78
11. Supplement: Layout of Beam and Experiment at NAL . .	80

### 3. Research Personnel

T. Erber: Professor of Physics,  
 Illinois Institute of Technology 1969-  
 BS (Physics)  
 Massachusetts Institute of Technology 1951  
 MS (Physics) University of Chicago 1953  
 PhD (Physics) University of Chicago 1957  
 Assistant Professor, Physics,  
 Illinois Institute of Technology 1957-1962  
 Associate Professor, Physics,  
 Illinois Institute of Technology 1962-1969  
 IIT Faculty Research Fellow, 1958-1959  
 Research Fellow, Universite Libre de Bruxelles, 1963-1964  
 Visiting Professor of Physics, University of Graz, 1971  
 Honorary Professor of Physics, University of Graz, 1971-

#### Publications since 1969

1. "Francis Bitter: Selected Papers & Commentaries," MIT Press,  
 x + pp. 551 (1969). [edited with C. M. Fowler]
2. "Study of a Magnetic Cooperative System," Acta Physica  
 Austriaca 30, 271-94 (1969). [with G. R. Marousek and G. K.  
 Forsberg]
3. "Idealized Treatment of Magnetic Flux Compression,"  
 Sitzungsberichte Oesterr. Akad. Wiss. Mathem.-naturw. Klasse  
178, 25-38 (1969). [with H. G. Latal and P. Urban]
4. "Electromagnetically Driven Flux Compression," Review of  
 Scientific Instruments 41, 1-7 (1970). [with F. Herlach  
 and D. Kachilla]
5. "Flux Compression Theories," Reports on Progress in Physics  
33, 1069-1127 (1970). [with H. G. Latal]

6. "The Origin of Hysteresis in Simple Magnetic Systems,"  
Advances in Chemical Physics 20, 71-134 (1971). [with H. G. Latal and B. N. Harmon]
7. "Probabilistic Metric Spaces and Hysteresis Systems,"  
Communications in Mathematical Physics 20, 205-219 (1971).  
[with B. Schweizer and A. Sklar]
8. "Force-Free Modes, Work-Free Modes, and Radiationless  
Electromagnetic Field Configurations," Acta Physica Austriaca  
32, 224-244 (1971). [with S. M. Prastein]
9. "Experiments with Megagauss Targets at SLAC," IEEE Trans.  
Nucl. Sci., NS-18, No. 13, pp.809-814 (1971). [with F.  
Herlach, R. McBroom, J. J. Murray, and R. Gearhart]
10. "Some External Field Problems in Quantum Electrodynamics,"  
Acta Physica Austriaca, Suppl.VIII, 323-357 (1971).
11. "A General Phenomenology of Hysteresis," Annals of Physics,  
69, 161-192 (1971). [with S. A. Guralnick and H. G. Latal]
12. "Statistical Theory of Magnetization in a Simple System,"  
Acta Physica Austriaca, 34, 313-330 (1971). [with H. G. Latal]
13. "Population Inversion in a Magnetic Condensation," Acta  
Physica Austriaca, 34, 345-350 (1971) [with H. G. Latal]
14. "Fourier Analysis of Flux Compression Fields," Acta Physica  
Austriaca, 34, 337-344 (1971).
- 15-17. "Analyses of Flux Compression Experiments, I,II,III," Acta  
Physica Austriaca (in press, 1972) [with J. E. Kennedy,  
H. G. Latal, and S. M. Prastein]
18. "Macroscopic Irreversibility as a Manifestation of Micro-  
Instabilities," Modern Developments in Thermodynamics, B.  
Gal-Or editor (in press 1972-73).[with A. Sklar]

19. "Mixing Transformations on Metric Spaces," Communications in Mathematical Physics (in press, 1973). [with B. Schweizer and A. Sklar]
20. "Breaking of Dilatational Symmetry of Dipole Interactions by Octupole Forces," Proc. Conf. on Magnetism and Magnetic Materials (in press, 1973). [with M. Duda, R. Olenick, and H. G. Latal]

<u>C. S. Shen:</u>	Associate Professor of Physics, Purdue University	1968-
	BS (Physics) Taiwan University	1957
	PhD (Physics) University of Maryland	1961
	Research Associate, Princeton University	1961-1962
	Research Associate, Institute for Space Studies	1962-1964
	Assistant Professor, Purdue University	1964-1966
	Visiting Associate Professor, Tsing Hua University, Republic of China	1966-1967
	Associate Professor, Purdue University	1968-
	Visiting Professor, Taiwan University and Tsing Hua University, Taiwan	1970-1971

### Publications

1. "Application of a Dispersion Relation to the Electron Impact Widths and Shifts of Isolated Spectral Lines from Neutral Atoms," Phys. Rev. 125, 196 (1962) [with H. Greim]
2. "An Analytic Solution for Density Distribution in a Planetary Exosphere," J. Atmospheric Sciences 20, 196 (1962).
3. "Thermionic Screening of Bodies in the Atmosphere and Interplanetary Space," J. Atmospheric Sciences 20, 359-365 (1963). [with K. P. Chopra]

4. "Density and Velocity Distributions in Exosphere," *Astronomical J.* 68, 79 (1963).
5. "The A.C. Conductivity of Plasma," *Plasma Phys.* 6, 389-399 (1964). [with R. L. W. Chen]
6. "Transit Acceleration of Charged Particles in an Inhomogeneous Electromagnetic Field," *Astrophys. J.* 141, 1091-1104 (1965).
7. "Photoelectric Screening of Objects Moving in an Ionized Medium," *AIAA J.* 3, 2337-2339 (1965). [with K. P. Chopra]
8. "Acceleration of Electrons Near the Magnetospheric Boundary," *Geophys. Union Transactions* 46, 135 (1965).
9. "Fermi Acceleration of Charged Particles in the Transition Region Beyond the Magnetosphere," *J. Geophys. Res.* 71, 241-251 (1966). [with C. C. Chang]
10. "The Effect of Weak Collisions on Ion Waves," *Phys. of Fluids* 9, 177-186 (1966). [with R. Kulsrud]
11. "Origin of High-Energy Electrons Beyond the Magnetosphere," *Nature* 211, 275-277 (1966). [with C. C. Chang]
12. "Possibility of Detecting Quarks Through Astronomical Observations," *Astrophysical J.* 147, 356-359 (1967). [with T. K. Kuo]
13. "Energy Spectrum and the Origin of Cosmic-Ray Electrons Above 12 BeV," *Phys. Rev. Letters* 19, 399-402 (1967).
14. "Cosmic Gamma Rays from Inverse Compton Scattering," *Astrophys. J.* 151, 895-900 (1968). [with G. Berkey]
15. "Solar Modulation of Galactic Cosmic Rays and Its Effect," *J. Geophys. Research* 73, 4273-4280 (1968). [with W. K. White]

16. "Antiprotons and Positrons in Cosmic Rays," Phys. Rev. 171, 1344-1348 (1968). [with G. B. Berkey]
  17. "High Energy Gamma Rays, Cosmic-Ray Electrons and the Far-Infrared Background Radiation," Phys. Rev. Letters 22, 568-572 (1969).
  18. "Pulsars and Ancient Chinese Records on Supernovae Explosions," Nature 221, 1039-1040 (1969).
  19. "Origin and Propagation of Cosmic-Ray Electrons," Phys. Rev. 188, (1969). [with G. B. Berkey]
  20. "Synchrotron Emission at Strong Radiative Damping," Phys. Rev. Letters 24, No. 8, 410-15 (1970).
  21. "Origin of Galactic Gamma Rays and a Two-Component Cosmic-Ray Model," Proce. XIth Intn'l Conf. on Cosmic Rays, published in Acta Phys. Acad. Scient. Hungaricae, 29, Suppl. 1, pp. 267-275 (1970).
  22. "Introduction to Astrophysics," Publ. 1968 (in Chinese, paperback book).
  23. "Recent Development in Astrophysics," Publ. 1970 (in Chinese, paperback book).
  24. "Pulsars and Very High-Energy Cosmic-Ray Electrons," Astrophys. J. 162, L181-L186 (1970).
  25. "Comment on the Synchrotron Motion with Radiation Damping," Phys. Rev. Letters 33A, 322 (1970).
  26. "Anisotropy of High Energy Cosmic-Ray Electrons in the Discrete Source Model," Astrophys. Letters 9, 169-174 (1971). [with W. C. Y. Mao]
-

27. "Energy Straggling and Radiation Reaction for Magnetic Bremsstrahlung," Phys. Rev. Letters 28D, No. 7, 455-459 (1972).
28. "Remarks on Relativistic Radiative Reaction," Intern. Jr. Theor. Phys. (in press).
29. "On the 'New' Equation of Motion for Classical Charged Particles," Phys. Rev. D (in press, 15 Nov. 1972).
30. "Magnetic Bremsstrahlung in an Intense Magnetic Field," Phys. Rev. D, 6 No. 10, 2736-54 (1972).

D. A. White: Post-Doctoral Research Fellow

BS (Physics)	Purdue University	1968
PhD (Physics)	Purdue University	1972

#### Publications

1. "Energy Straggling and Radiation Reaction for Magnetic Bremsstrahlung," Phys. Rev. Letters 28, No. 7, 455-9 (Feb. 1972). [with C. S. Shen]
2. "Quantum Mechanical Treatment of an Electron Undergoing Synchrotron Radiation," Phys. Rev. D5, No. 8, 1930-36, (April 1972).
3. "The Second Order Correction to the First Order Quantum Mechanical Treatment of an Electron Undergoing Synchrotron Radiation," Phys. Rev. D (15 Oct. 1972, in press).

#### Graduate Students

P. Everett	R. Olenick
E. Kinzel	

#### Additional Personnel

The experiments will be carried out in collaboration with



the following senior personnel:

Dr. H. H. Heckman, Lawrence Berkeley Laboratory

Dr. H. G. Latal, University of Graz

#### 4. Magnetic Bremsstrahlung

##### (a) Radiation Reaction Effects [Uniform Fields]

Radiation reaction enters electrodynamics through the logical necessity of balancing the energy-momentum conservation laws. However the precise calculation of this effect is clouded with ambiguity since the conservation laws only furnish constraints and do not lead to any specific equations of motion. Additional assumptions must be made and these lead to a variety of dynamical possibilities. The most famous and widely accepted is the Lorentz-Dirac equation:

$$\dot{u} = \omega_{\mu\nu} u^\nu + \frac{2e^2}{3mc^3} \left\{ \ddot{u}_\mu - \frac{1}{c^2} u_\mu \dot{u}^\nu \dot{u}_\nu \right\}, \quad (4.1)$$

where  $u_\mu$  is the four-velocity, the dots indicate proper time derivatives; and we shall specialize to the case where the external forces are derived from the electromagnetic field tensor, viz.

$$\omega_{\mu\nu} = \frac{e}{mc} \begin{vmatrix} 0 & H_z & -H_y & E_x \\ -H_z & 0 & H_x & E_y \\ H_y & -H_x & 0 & E_z \\ -E_x & -E_y & -E_z & 0 \end{vmatrix} \quad (4.2)$$

Extensive reviews of the problems associated with the derivation of this equation, the identification of physically meaningful

solutions (the "runaway" problem), and the merits of other dynamical principles are given in [11] and [20]. New alternatives are frequently proposed in the literature, e.g. reference [21].

A non-trivial test of (4.1) requires conditions where radiation reaction is a "strong" effect. A good diagnostic is the ratio of the rate of momentum transfer to the radiation field to the rate of momentum transfer associated with the external forces, e.g. the elastic scattering of electrons by a magnetic field. This ratio is given by [12], [19]

$$R_c = \frac{2}{3} \alpha \left( \frac{E}{mc^2} \right)^2 \left( \frac{H}{H_{cr}} \right), \quad (4.3a)$$

or in practical units

$$R_c = 4.16 \times 10^{-4} E^2 (\text{GeV}) H (\text{MG}). \quad (4.3b)$$

Table 2 shows that the SLAC-IIT experiments were the first in which strong radiation reaction conditions corresponding to  $R_c \sim 1$  were reached. Obviously the NAL experiments would extend this range much further. The general situation --- including pulsar conditions --- is mapped out on Fig. 1.

Table 2. Values of the Radiation Reaction Parameter  $R_c$

Experiment	DESY [22]	SLAC-IIT	NAL-IIT (Phase I)	NAL-IIT (Phase II)	NAL-IIT (Phase IV)
E (GeV)	6	19	150	300	300
H (MG)	0.006	1.6	2	3	7
$R_c$	$10^{-4}$	0.24	18.7	112	262

Closed form solutions of (4.1) for the motion of charged particles in a uniform magnetic field are not available. Due to the "run-away" pathologies inherent in (4.1) straightforward numerical integrations cannot be applied [23]. Furthermore under experimental conditions which violate the inequality  $R_c \ll 1$ , simple perturbation expansions, such as those of Plass [24] and Arzeliès [25], lose their validity. The first plausible calculations of the effects to be expected for  $R_c \gtrsim 1$  were reported in [1] and [2]. The essential idea is to transform (4.1) to the instantaneous rest system. One can then evaluate the 4-acceleration by expanding in powers of the dimensionless ratio  $\frac{mc^2}{E} R_c$ , which remains a small quantity even for the range of conditions listed in Table 2. Relativistic invariance then assures the equivalence

$$\begin{aligned}
 (\ddot{u}^j \ddot{u}_j)_{\text{Lab}} = (\ddot{u}^j \ddot{u}_j)_{\text{Rest}} \approx & \left( \frac{c}{\hbar} \frac{EH}{H_{\text{cr}}} \sin \phi \right)^2 \left\{ 1 + \left( \frac{2\alpha}{3} \frac{E}{mc^2} \frac{H}{H_{\text{cr}}} \right)^2 \right. \\
 & \left. + \frac{4\alpha\hbar}{3mc^2} \frac{\dot{E}}{E \sin^2 \phi} - \left( \frac{mc^2}{E \sin \phi} \right)^2 + \mathcal{O} \left[ \left( \frac{mc^2}{E} R_c \right)^4 \right] \right\},
 \end{aligned}
 \tag{4.4}$$

where  $\alpha^{-1} = '137'$ ,  $H_{\text{cr}} = \frac{m^2 c^3}{e\hbar} \approx 4.414 \times 10^{13} \text{ G}$ , and  $\phi$  is the angle between  $\vec{v}$  and  $\vec{H}$ . Substituting into (4.1) and integrating yields the time dependence of the velocity:

$$\begin{aligned}
 v_x(t) &= v_0 e^{-h(t)} \cos [f(t)] \sin \phi_0, \\
 v_y(t) &= v_0 e^{-h(t)} \sin [f(t)] \sin \phi_0, \\
 v_z(t) &= v_0 \cos \phi_0;
 \end{aligned}
 \tag{4.5}$$

where  $\phi_0$  is the angle between  $\vec{v}$  and  $\vec{H}$  at  $t = 0$ ,  $\vec{H}$  is directed along the z-axis, and  $v_y(0) = 0$ . The auxiliary functions  $h(t)$  and  $f(t)$  are given by

$$h(t) \approx \frac{2\alpha}{3} \frac{mc^2}{E_0} \left( \frac{H}{H_{cr}} \right)^2 \frac{ct}{\lambda_c} \sin \phi_0 \left\{ 1 + \frac{\alpha}{3} \frac{E_0}{mc^2} \left( \frac{H}{H_{cr}} \right)^2 \frac{ct}{\lambda_c} \sin \phi_0 \right\}, \quad (4.6a)$$

and

$$f(t) \approx \frac{mc^2}{E_0} \frac{H}{H_{cr}} \frac{ct}{\lambda_c} \left\{ 1 + \frac{\alpha}{3} \frac{E_0}{mc^2} \left( \frac{H}{H_{cr}} \right)^2 \frac{ct}{\lambda_c} \sin \phi_0 \right\}; \quad (4.6b)$$

where  $\lambda_c$  is the (electron) Compton wavelength, and the subscript "o" denotes the initial values at  $t = 0$ . We note in passing that for practical MG-targets  $ct/\lambda_c \sim 10^{10}$ .

If we now consider the passage of a charged particle through a uniform magnetic field, then after path length  $L$ , the particle will be deflected through an angle

$$\theta \approx f(t) \equiv \theta_0 + \delta\theta_{CD}, \quad (4.7a)$$

where

$$\theta_0 = \frac{mc^2}{E_0} \frac{H}{H_{cr}} \frac{L}{\lambda_c}, \quad (4.7b)$$

is the ordinary "elastic" scattering due to the Lorentz force, and

$$\delta\theta_{CD} = \frac{\alpha}{3} \left( \frac{H}{H_{cr}} \right)^3 \left( \frac{L}{\lambda_c} \right)^2 \sin \phi_0 \quad (4.7c)$$

is an additional deflection which is caused by the radiation damping. In practical units

$$\delta\theta_{CD}(\text{mrad}) = 1.90 \times 10^{-4} H^3(\text{MG}) L^2(\text{mm}), \quad (4.7d)$$

which coincides with the basic relation (1) given in the Summary. The following properties of (4.7c) are useful from an experimental point of view:

- (i)  $\delta\theta_{CD}$  is odd under charge conjugation; this implies that the damping always increases the deflection. Since radiative losses decrease the particle's rigidity, this is an obvious requirement.
- (ii)  $\delta\theta_{CD}$  varies with the inverse fourth power of the mass of the radiating particle. In view of (4.7d) the radiative shifts are negligible for all particles except electrons ( $e^\pm$ ).
- (iii)  $\delta\theta_{CD}$ , in first approximation, is independent of the energy.

The technical problems associated with the straightforward detection and measurement of (4.7c) are discussed in Section 5.

Here we would like to note briefly that (ii) and (iii) lend themselves to an elegant differential experiment: Suppose that a mixed pulse of essentially monoenergetic pions and electrons were directed at the MG target during the  $2 \mu\text{sec}$  rise time of the field. The variation in the deflection due to "elastic" scattering is then strictly linear with the field-path (integral), i.e.

$$\theta_o^\pi - \theta_o^e = eHL \left( \frac{E_o^e - E_o^\pi}{E_o^e E_o^\pi} \right). \quad (4.8)$$

However the experimentally observable difference in the scattering angles is given by

$$|\theta(\pi) - \theta(e)|_{\text{exp}} = (\theta_o^\pi - \theta_o^e) + \delta\theta_{CD} \text{ (electrons only!)}, \quad (4.9)$$

where the second term has a non-linear dependence on the field-path integral. The dominance of the radiative effects is then equivalent to the condition

$$\delta\theta_{CD} \gtrsim \theta_0^\pi - \theta_0^e. \quad (4.10a)$$

In practical units this corresponds to

$$H^2(\text{MG}) L(\text{mm}) \gtrsim 15.7 \times 10^4 \left( \frac{E_0^e - E_0^\pi}{E_0^e E_0^\pi} \right)_{\text{GeV}}. \quad (4.10b)$$

One can easily check that for  $E_0^e - E_0^\pi \sim 1 \text{ GeV}$ ,  $E_0^e \sim 200 \text{ GeV}$ , the damping effects dominate (4.9) even for conservatively designed MG-targets. However, more important is the fact that since the  $e$  and  $\pi$  pulses pass through the MG targets simultaneously, the essential jitter is localized in the  $E_0^e$ ,  $E_0^\pi$  variations within a single  $2 \mu\text{sec}$  machine burst. For this we can conservatively assume

$$\frac{\Delta E_0^e}{E_0^e} \approx \frac{\Delta E_0^\pi}{E_0^\pi} \approx 1\%. \quad (4.10c)$$

The elastic component of (4.9) therefore has at most a jitter of the order of 2%; and an unambiguous measurement of  $\delta\theta_{CD}$  should be possible. In practice one would display both the  $e$  and  $\pi$  deflections on emulsions and provide the time resolution by following the MG target (horizontal dispersion) with a pulsed magnet (vertical dispersion).

A DC-approximation of this arrangement has already been tried successfully during the SLAC-IIT experiments. The final result should be an emulsion record resembling a slanted letter

" $\gamma$ ": the progressive spread of the limbs is due to  $\delta\theta_{CD}$  and should vary with  $H^3$ . (One limb will also be smeared due to energy straggling effects [Section 4c].) The difference in the H and L dependence of (4.7b) and (4.7c) is of course also useful in a number of applied situations where an independent determination of their variation is desired.

(b) Radiation Reaction Effects [Non-Uniform Fields]

Follow up studies of the SLAC-IIT experiments have shown that the field inhomogeneities of the MG coils have the following properties:

- (1) The spatial field variation over the central millimeter is  $\frac{\Delta H}{H} \sim 0.003$ , over the central two millimeters  $\frac{\Delta H}{H} \sim 0.02$ ; corresponding to a total coil diameter of 5 mm.
- (2) The uncertainty in the determination of  $\int H d\ell$  is less than 1%.
- (3) Magnetic field inhomogeneities are localized near the MG target beam holes; gradients of the order of 1 MG/mm may occur in this region.
- (4) The maximum time variation of H in a  $0.3 \mu\text{sec}$  window centered on the field peak is  $|\dot{H}| \lesssim 0.2 \text{ MG}/\mu\text{sec}$ .

Clearly it is necessary to show that in any practical experimental set up the perturbations due to these field inhomogeneities are negligible compared to (4.7d). We have therefore extended the radiation reaction theory sketched in the previous Section to include the effects of spatial and temporal field variations. We shall present here a brief outline of the arguments which lead to concise analytical upper bounds. These confirm that MG targets

of the kind used at SLAC will permit accurate measurements of the radiation reaction effects. Of course, for the NAL experiments, we will adapt the theory for computer evaluation --- this will replace the analytical upper bounds with precise numbers.

We begin again with the Lorentz-Dirac equation (4.1), and now make the following specific ansatz for the electromagnetic fields (4.2):

$$\vec{H} = (\epsilon H_1, \epsilon H_2, H_3),$$

and

(4.11)

$$\vec{E} = (\epsilon E_1, \epsilon E_2, \epsilon E_3); \quad "1" = x, "2" = y, "3" = z.$$

As before  $H_3$  is the principal megagauss field --- however in the present instance we shall make allowance for the fact that it may have gradients.  $H_1$  and  $H_2$  represent field inhomogeneities associated with the beam holes in the MG-targets. The electric fields arise from the time variation of  $H$ ,

$$\nabla \times \vec{E} = - \frac{1}{c} \frac{\partial \vec{H}}{\partial t}. \quad (4.12)$$

For ease of calculation we assign the same parameter of smallness  $\epsilon$  to scale each of the perturbing fields. The basic equation of motion then is

$$\dot{U}_i = \frac{e}{mc} F_{ik} U^k + \frac{1}{\omega_0} \left( \ddot{U}_i - \frac{1}{c^2} U_i \dot{U}^k \dot{U}_k \right), \quad (4.13)$$

where  $F_{ik}$  is the field tensor,  $U_i$  is the 4-velocity, dots indicate differentiation with respect to proper time, and  $\omega_0 = 3mc^3/2e^2$ . Since the internal consistency of electrodynamics is limited to field strengths satisfying



$$\frac{E}{mc^2} \frac{|F_{ik}|}{F_{cr}} \ll 1, \quad F_{cr} = \frac{m^2 c^3}{e \hbar}; \quad (4.14)$$

we can expand (4.13) in powers of

$$\frac{\gamma e |F_{ik}|}{\omega_0 mc}$$

where  $\gamma = [1 - \beta^2]^{-1/2}$ , and  $\beta = v/c$ . To lowest order we find

$$\dot{U}_i = \frac{e}{mc} F_{ik} U^k + K U_i, \quad (4.15)$$

where the radiation reaction term is scaled by the factor

$$K = - \frac{e}{mc} F_{lj} \dot{U}^j U^l = \frac{2\gamma^2 e^4}{3m^3 c^5} \left\{ [\vec{\beta} \times \vec{H} + \vec{E}]^2 - (\vec{E} \cdot \vec{\beta})^2 \right\}. \quad (4.16)$$

Note that (4.14) does not preclude the circumstance that the radiation reaction term in (4.15) may dominate the Lorentz force.

We now insert the fields (4.11) into (4.13), and as before exploit the fact that  $\dot{U}_i U^i = 0$ , and  $\dot{U}_i \dot{U}^i$  is an invariant. The solutions of the resulting coupled differential equations can be developed in power series of  $\epsilon$  through iteration methods. After translating the covariant quantities to the space and time variables appropriate to the laboratory, we find to the lowest order in  $\epsilon$  and  $\gamma^{-1}$

$$\begin{aligned} \gamma(t) = \gamma_0 \left\{ \int_0^t E_1 v_0 \sin \phi_0 \cos A(t', 0) e^{-B(t')} dt' \right. \\ - \int_0^t E_2 v_0 \sin \phi_0 \sin A(t', 0) dt' \\ \left. + \int_0^t E_3 v_0 \cos \phi_0 dt' \right\} \end{aligned} \quad (4.17)$$

where

$$\gamma(t) = \gamma_0 (1 + \gamma_0 / \omega_0 \int_0^t \omega_{H3}^2 dt')^{-1} + \epsilon I_0, \quad (4.18a)$$

$$v_1(t) = v_{10} \cos A(t, 0) + \epsilon I_1, \quad (4.18b)$$

$$v_2(t) = -v_{10} \sin A(t, 0) + \epsilon I_2, \quad (4.18c)$$

$$v_3(t) = v_{30} + \epsilon I_3; \quad (4.18d)$$

and the auxiliary I functions are given by

$$I_0 = \frac{e}{mc^2} \int_0^t dt' [E_1 v_{10} \cos A(t', 0) + E_2 v_{10} \sin A(t', 0) + E_3 v_{30}] \quad (4.19a)$$

$$I_1 = \frac{e}{mc} \int_0^t dt' [(E_1 c - H_2 v_{30}) \cos A(t, t') + (E_2 c + H_1 v_{30}) \sin A(t, t')] / \gamma(t') \quad (4.19b)$$

$$I_3 = \frac{e}{mc} \int_0^t dt' [H_1 v_{10} \sin A(t', 0) + H_2 v_{10} \cos A(t', 0) + E_3 c] / \gamma(t') \quad (4.19c)$$

and

$$A(t, t') = \frac{e}{mc} \int_{t'}^t H_3 / \gamma dt'' \quad (4.19d)$$

The coordinates are chosen so that at  $t = 0$  the particle enters the field with  $\vec{v} = (v_{10}, 0, v_{30})$ . This makes explicit allowance for misalignment of the beam and the pulsed MG fields. To find the trajectory of the particle one has to carry out another quadrature in eqs. (4.18a,d). However, the effects of the field variation on the deflection angle  $\theta$  can be estimated directly from the velocity functions, i.e.

$$\theta = \tan^{-1} \left| \frac{v_2}{v_1} \right| \approx \tan^{-1} \left\{ \tan A(t,0) \left[ 1 - \epsilon I_1/v_{10} \cos A(t,0) - \epsilon I_2/v_{10} \sin A(t,0) \right] \right\}. \quad (4.20)$$

Once the actual field profile is known (4.20) can be used to calculate the deflection angle through numerical integration.

We shall consider two simple special cases to illustrate the essential features. Suppose first we assume

$$(i) \quad \vec{E} = 0, \quad \vec{H} = (0,0, H_0 x/x_0).$$

This represents the case of a particle that is injected into a magnetic field with a constant gradient. From (4.20) we find

$$\theta(t) = \int_0^t \frac{eH_0}{\gamma_0 mc} \left[ 1 + \frac{\gamma_0 e^2 H_0^2}{\omega_0 m^2 c^2} \int_0^{t'} \frac{x^2(x'')}{x_0^2} dt'' \right] \frac{x(t')}{x_0}. \quad (4.21)$$

In particular, for small deflections, this reduces to

$$\theta(x) = \frac{eH_0 x^2}{2 \gamma_0 mc v_{10} x_0} \left( 1 + \frac{4}{45} \frac{\gamma_0 e^4 H_0^2 x^3}{m^3 c^5 v_{10} x_0^2} \right). \quad (4.22)$$

If we compare with the deflection in a uniform magnetic field  $H$ , i.e.

$$\theta(x) = \frac{eHX}{\gamma_0 mc v_{10}} \left( 1 + \frac{1}{3} \frac{\gamma_0 e^4 H^2 x}{m^3 c^5 v_{10}} \right), \quad (4.23)$$

we find, as expected, that the modified deflection is essentially given by replacing  $H$  with the average field

$$\langle H(x) \rangle = \frac{1}{x} \int_0^x H(x) dx = \frac{1}{2} \frac{H_0 x}{x_0} \quad (4.24)$$

in (4.23). There are no anomalous effects associated with the occurrence of steep gradients. By similar analysis one can

easily show that this conclusion also applies to fields with a constant rate of time variation.

(ii) As a second example we shall consider a set of fields which are constant in space and time, i.e.  $\vec{E} = \epsilon(E_1, E_2, E_3)$ ,  $\vec{H} = (\epsilon H_1, \epsilon H_2, H_3)$ . For small deflection we have

$$\theta \approx A(t, 0) - \epsilon I_2 / v_{10}. \quad (4.25)$$

Explicit evaluation of (4.19 c & d) then gives

$$\begin{aligned} A(t, 0) &= \frac{eH_3}{mc} \int_0^t dt' / \gamma(t') \\ &= \frac{eH_3 t}{\gamma_0 mc} \left[ \left( 1 + \frac{\gamma_0 e^4 H_3^2 t}{3m^3 c^5} \right. \right. \\ &\quad \left. \left. - \epsilon \frac{e\vec{E} \cdot \vec{v}_0 t}{2\gamma_0 mc^2} \left( 1 + \frac{8}{9} \frac{\gamma_0 e^4 H_3^2 t}{m^3 c^5} + \frac{2}{9} \frac{\gamma_0^2 e^8 H_3^4 t^2}{m^6 c^{10}} \right) \right] \right] \quad (4.26a) \end{aligned}$$

and

$$I_2 = A(t, 0) (E_2 c + H_1 v_{30}) / H_3. \quad (4.26b)$$

The corresponding deflection is

$$\begin{aligned} \theta(x) = \theta_0(x) &\left\{ \left( 1 + \frac{1}{2} R_0 \theta_0(x) - \epsilon \left[ \frac{e\vec{E} \cdot \vec{v}_0 x}{2\gamma_0 mc^2 v_{10}} + \frac{E_2 c + H_1 v_{30}}{H_3 v_{10}} \right. \right. \right. \\ &\quad \left. \left. + \frac{R_0 \theta_0(x)}{2} \left( \frac{4e\vec{E} \cdot \vec{v}_0 x}{3\gamma_0 mc^2 v_{10}} + \frac{E_2 c + H_1 v_{30}}{H_3 v_{10}} \right) \right] \right\}, \quad (4.27) \end{aligned}$$

where

$$\theta_0(x) = \frac{eH_3 x}{\gamma_0 mc v_{10}} \approx 0.3 H(\text{MG}) X(\text{cm}) / E(\text{GeV}), \quad (4.28a)$$

is the ordinary "elastic" scattering [cf. (4.7b)], and

$$R_0 = \frac{2 \gamma_0^2 e^3 H_3}{3 m^2 c^4} \sim 4 \times 10^{-4} E^2(\text{GeV}) H(\text{MG}), \quad (4.28b)$$

indicates the strength of the radiation reaction [cf. (4.3b)]. The structure of (4.27) clearly displays the fact that  $\theta_0$  is modified by a term proportional to  $R_0$ , which represents the corrections due to radiation damping, and a term proportional to  $\epsilon$ , which represents the combined effects of all perturbing fields.

We can now allow for space-time fluctuations of the perturbing fields by combining cases (i) and (ii). The net result is that the perturbing fields in (4.27) are replaced by the average values, i.e.  $\langle \vec{E}(\vec{r}, t) \rangle$  and  $\langle \vec{H}(\vec{r}, t) \rangle$ . This is the general case that is required for estimating the interference between radiation damping and the defocussing effects of the perturbing fields. Suppose we rewrite (4.27) in the form

$$\theta(x) = \theta_0(x) + \delta\theta_{CD} + \delta\theta_\epsilon, \quad (4.29a)$$

where  $\delta\theta_\epsilon$  represents the deflections due to the perturbing fields. Then to first order

$$\frac{\delta\theta_\epsilon}{\delta\theta_{CD}} = \left\langle \left[ \frac{e\vec{E} \cdot \vec{v}_0 x}{2\gamma_0 m c^2 v_{10}} + \frac{E_2 c + H_1 v_{30}}{H_3 v_{10}} \right] \left[ \frac{3m^3 c^5 v_{10}}{e^4 H_3^2 x \gamma_0} \right] \right\rangle. \quad (4.29b)$$

For megagauss experiments whose main purpose it is to measure radiation reaction effects, we clearly want to adjust conditions so that

$$\delta\theta_\epsilon \ll \delta\theta_{CD}. \quad (4.30a)$$

From (4.29b) we can then readily derive a set of sufficient constraints:

$$\frac{\epsilon \langle E_x \rangle}{\langle H_z \rangle} \ll 4.2 \times 10^{-4} E_0^2 (\text{GeV}) H (\text{MG}) \quad (4.30b)$$

$$\frac{\epsilon \langle E_y \rangle}{\langle H_z \rangle} \ll 0.62 \times 10^{-5} E_0 (\text{GeV}) H^2 (\text{MG}) L (\text{mm}) \quad (4.30c)$$

$$\frac{\epsilon \langle H_x \rangle}{\langle H_z \rangle} \ll 0.62 \times 10^{-5} E_0 (\text{GeV}) H^2 (\text{MG}) L (\text{mm}) / \Delta \theta_v, \quad (4.30d)$$

where  $\langle H_z \rangle \sim H$  is the principal (megagauss) field,  $E_0$  is the particle's initial energy,  $L$  is the effective path length in the MG-target, and  $\Delta \theta_v$  is the incident vertical beam divergence (Table 1). Clearly (4.30c) imposes the tightest requirements. However from the estimates of the field variations given in (4) at the beginning of this Section, we can infer

$$\frac{\epsilon \langle E_y \rangle}{\langle H_z \rangle} \lesssim \frac{L}{c} \frac{\langle \dot{H}_z \rangle}{\langle H_z \rangle} \sim 10^{-4} \ll 2 \times 10^{-2}, \quad (4.30e)$$

where the last bound corresponds to the conservative assumptions  $E_0 \sim 150$  GeV,  $H \sim 2$  MG, and  $L \sim 5$  mm. The perturbing fields will therefore not obscure the radiation reaction shifts.

### (c) Quantum Fluctuation Effects

It is expected that under conditions of high momentum transfer quantum effects will appreciably influence the characteristics of magnetic Bremsstrahlung. The classical theory may therefore be considered reliable only under circumstances where the ratio of the photon to the electron momentum is essentially negligible.

A rough criterion for this is

$$\Upsilon = \frac{E}{mc^2} \frac{H}{H_{cr}} \approx 4.43 \times 10^{-5} E(\text{GeV}) H(\text{MG}) \ll 1. \quad (4.31)$$

It is however known that at high energies relativistic effects enhance the influence of quantum corrections. In particular it has been shown by Schiff [26] that the general inequality (4.31) should be replaced by the stricter condition

$$\Upsilon^{1/2} \ll 1.$$

This is only marginally satisfied for the range of parameters available for the NAL experiments, and indicates that if one only looks in the right places then the transition to the quantum regime can be measured quite accurately. The modifications in the Bremsstrahlung spectrum and total radiation rates are given by eqs. (3) - (5). Detailed calculations are carried out in [27] and [19]. As indicated previously we plan to postpone experimental checks of these features until the NAL set-up has been augmented by appropriate counting equipment (Phase II).

In the present Section we would like to call attention to the fact that there is another quantum effect which will show up quite markedly in the electron "elastic" scattering, and which therefore can be conveniently studied with the same emulsion techniques that will be used to measure the radiation damping shifts [3], [12]. This point can be best explained by comparing the physical meaning of radiation reaction in the quantum mechanical calculation and that in the classical calculation. In classical electrodynamics an accelerated particle loses energy continuously, thus both the damping of the particle's

energy and the modification of the radiation process due to the radiation reaction effectively constitute a feed back loop [11].

Neglecting the reaction force  $\omega_o^{-1} (\ddot{U}_1 - \frac{1}{c^2} \dot{U}^k \dot{U}_k)$  in the Lorentz-Dirac equation would make the radiating electron move with constant energy, violating the energy conservation law. In the quantum mechanical treatment, the radiation consists of discrete steps. A particle stays in a state for a finite time before making a transition to a lower state. Since the life time in a given energy state is very short ( $\tau = \frac{1}{\alpha} \frac{\hbar}{mc^2} \frac{H_{cr}}{H}$ ), a particle usually makes a number of transitions during the time of observation. If one follows the transition step by step, i.e., after the first emission, the radiated photon energy is subtracted from the initial electron energy, and the reduced energy is used in the calculation of the second emission process, and so on, then the final results will automatically include the damping effect. Such a cascade calculation has already been carried out. In addition to the inclusion of the effect of radiation damping, a statistical phenomenon due to the discrete nature of quantum transitions appears. Under certain conditions the broadening in energy states due to statistical fluctuations may reach a magnitude comparable to the shift caused by the radiation damping. We shall estimate its effect here.

Let  $\rho(E, t)$  be the number of electrons in the states within the energy range  $E$  and  $E + dE$ . We have

$$\frac{\partial \rho(E, t)}{\partial t} = - \frac{1}{\tau(E)} \rho(E, t) + \int_0^\infty \lambda(E, E') \rho(E', t) dE'. \quad (4.32)$$



Since the individual transition probabilities  $\lambda(E, E')$  are known [27], Eq. (4.32) can be solved by straightforward numerical methods [4]. The solution  $\rho(E, t)$  describes the energy distribution of the particles at time  $t$  with initial distribution  $\rho(E, 0)$ . Observables such as the expected instantaneous radiation spectrum can be readily calculated from  $\rho(E, t)$  by  $I(\omega, t) = \int \rho(E, t) I(\omega, E) dE$ . The spread in energy states is analogous to the energy straggling which occurs when a fast particle travels through a thickness of matter. The only difference being that in ordinary Coulomb Bremsstrahlung the spectrum of the radiation emission is nearly flat, hence the straggling is fairly insensitive to the initial energy of electron. In synchrotron emission the maximum fractional energy carried away by an individual quantum is characterized by  $\Upsilon(1 + \Upsilon)^{-1}$  [see (4.31)], thus the straggling effect is appreciable only when  $\Upsilon$  is not negligibly small.

To illustrate the relative magnitude of the fluctuation effect and the damping effect we present a quantum mechanical calculation of the deflection angle of an electron traversing through a strong magnetic field. The rate of change of direction for a particle in the eigenstate  $(N_1, S_1)$  ( $N_1$  is the principle quantum number, which determines the energy and the radius of the curvature, and  $S_1$  is the radial quantum number which characterizes the position of the center of the trajectory) is

$$\frac{d\theta_1}{dt} = \frac{v}{r(N_1, S_1)}, \quad (4.33)$$

where

$$r(N_i, S_i) = \langle \Psi_{N_i, S_i} | r | \Psi_{N_i, S_i} \rangle = N_i^{1/2} r_H [1 + (S_i + 1/2)/4N_i], \quad (4.34)$$

and  $r_H = (2H_q/H)^{1/2} \hbar/mc$  is the "Bohr radius" of an electron in a magnetic field. The total deflection of the electron after traversing a distance  $L$  in a magnetic field  $H$  is

$$\theta = \sum_{i=1}^m \frac{(t_i - t_{i-1})v}{r(N_i - S_i)} \quad (4.35)$$

where  $t_i$  is the instant the particle makes the transition from state  $(N_i, S_i)$  to state  $(N_{i+1}, S_{i+1})$ ,  $t_0$  is the time the particle enters the field, and  $t_m = L/c$  is the time the particle leaves the field. The duration  $(t_i - t_{i-1})$  which is the length of time the particle stays in the  $i$ th state and the probability that it will decay to the  $i+1$  state are both governed by the transition probability  $\lambda_{N_i, S_i, N_{i+1}, S_{i+1}}$ . To evaluate  $\theta$  let us first

consider the factor  $(S_i + 1/2)/4N_i$  in Eq. (4.34). As has been shown by Sokolov and Ternov [27] and Urban and Wittmann [28] the quantum number  $S$  is an increasing function of time

$$\begin{aligned} \frac{\Delta S}{\Delta t} &= \int \sum_j (S_j - S_i) \lambda_{N_i, S_i, N_j, S_j} dN_j \\ &= \frac{55}{48\sqrt{3}} \gamma^4 e^4 H^2 / m^3 c^5. \end{aligned} \quad (4.36)$$

Because the radiation processes do not involve a change of the radial quantum number,  $S$  increases linearly with time irrespective of the level transitions. (This is a distinct effect which is the cause of betatron oscillations in accelerators!)

After traversing a distance  $L_i$ ,

$$\begin{aligned} \frac{S(L_i)}{4N_i} &= \frac{S(0)}{4N_i} + \frac{55}{216\sqrt{3}} \alpha \Upsilon^2 (L_i/\lambda) (H/H_q) \\ &\approx \frac{S(0)}{4N_i} + 10^{-8} H^3 (\text{MG}) E^2 (\text{GeV}) L_i (\text{cm}). \end{aligned} \quad (4.37)$$

If we chose the coordinate such that the center of the orbit coincides with the origin when the electron enters the field, and the S-dependent fluctuation correction  $\delta_S = \frac{55}{216\sqrt{3}} \alpha \Upsilon^2 (L/\lambda) (H/H_q)$  is small compared to unity, then the total deflection may be expressed by

$$\theta = \theta_m (1 - \delta_S) \quad (4.38a)$$

where

$$\theta_m = \sum_{i=1}^m \frac{v(t_i - t_{i-1})}{N_i^{1/2} r_H}. \quad (4.38b)$$

The quantum spread  $\theta_m$  can be calculated by Monte-Carlo methods. The distribution of the deflection angles for a beam of monochromatic (energy) electrons after traversing a distance in  $H$  is shown in Figs. 2, 3, and 4 for a representative range of parameters. In case  $\Upsilon \ll 1$ , an adequate formula for  $\langle \theta \rangle$ , the average quantum mechanical deflection angle is

$$\langle \theta \rangle \approx \left[ 1 + \frac{R_c e H_L}{2 E_0} (1 - 4\Upsilon + 21\Upsilon^2) \right] \frac{e H L}{E_0}. \quad (4.39)$$

The angular spread of the particles due to quantum fluctuations is scaled by the mean deviation

$$\Delta \theta_{QM} = \left[ \langle \theta^2 \rangle - \langle \theta \rangle^2 \right]^{1/2}. \quad (4.40)$$

The approximate formula for this spread is

$$\Delta \theta_{QM}(\text{mrad}) \cong \frac{0.95 \times 10^{-3} H^{5/2}(\text{MG}) L^{3/2}(\text{mm})}{1 + 1.33 \times 10^{-5} H^2(\text{MG}) L(\text{mm}) E_0(\text{GeV})}. \quad (4.41)$$

Estimates based on (4.41) agree closely with numerical results derived from Monte-Carlo calculations.

For completeness sake we note that (4.39) can be generalized to include other quantum mechanical modifications of the "elastic" scattering angle, viz.

$$\langle \theta \rangle = \theta_0 + \delta \theta_{CD} + \delta \theta^{(1)} + \delta \theta^{(2)}, \quad (4.42a)$$

where the individual terms have the following significance [28], [12]:

$$\theta_0 = \text{the ordinary Lorentz deflection (4.7b)}, \quad (4.42b)$$

$$\delta \theta_{CD} = \text{additional deflection due to radiation damping (4.7c)}, \quad (4.42c)$$

$$\delta \theta^{(1)} = - \frac{715 \alpha}{192 \sqrt{3}} \frac{L}{\lambda_c} \left( \frac{E_0}{mc^2} \right)^2 \left( \frac{H}{H_{cr}} \right)^3 \theta_0, \quad (4.42d)$$

(quantum correction of  $\delta \theta_{CD}$ )

$$\delta \theta^{(2)} = - \frac{1}{2} \langle S_0 \rangle \theta_0 \left( \frac{mc^2}{E_0} \frac{H}{H_{cr}} \right) \left[ \frac{mc^2}{E_0} + \right. \\ \left. + \frac{\alpha}{3} \frac{L}{\lambda_c} \left( \frac{H}{H_{cr}} \right)^2 \left\{ 1 - \frac{55 \sqrt{3}}{16} \frac{E_0}{mc^2} \frac{H}{H_{cr}} \right\} \right], \quad (4.42e)$$

(betatron effect)

Due to the well known degeneracy of the orbit centers,  $\langle S_o \rangle$  is not a sharply defined quantity: Its order of magnitude is given by

$$\langle S_o \rangle \sim \frac{\overline{\Delta r}}{\lambda_c} \left[ \frac{H}{H_{cr}} \right]^{1/2}, \quad (4.42f)$$

where  $\overline{\Delta r}$  is the initial spatial spread of the beam ( $\sim 1$  mm).

If we insert plausible parameter values, it becomes clear that the statistical spread (4.41) is the most important quantum effect.

As indicated in the Project Summary, Phase I will concentrate on the measurement of  $\delta\theta_{CD}$  and  $\Delta\theta_{QM}$ . This is schematically indicated on Fig. 5. A summary of representative values is given in Table 3.

Table 3. Radiation Reaction Shifts and Quantum Straggling

E(GeV)	H(MG)	L(mm)	$\theta_o$ (mrad) (4.7b)	$\delta\theta_{CD}$ (mrad) (4.7c)	$\Delta\theta_{QM}$ (mrad) (4.41)
150	1.5	5	1.5	0.016	0.028
300	1.5	5	0.75	0.016	0.028
150	1.5	10	3.0	0.064	0.078
300	1.5	10	1.5	0.064	0.075
150	2	5	2	0.038	0.047
300	2	5	1	0.038	0.045
150	2	10	4	0.15	0.13
300	2	10	2	0.15	0.12
150	2.5	5	2.5	0.074	0.098
300	2.5	5	1.25	0.074	0.093
150	2.5	10	5	0.30	0.26
300	2.5	10	2.5	0.30	0.24
150	3	10	6	0.51	0.40
300	3	10	3	0.51	0.34

## (d) Compton Scattering and Soft Photon Emission

It has been pointed out previously that binding effects can enormously enhance the cross-sections for magnetic Compton scattering [19]. Preliminary results of a quantum mechanical calculation of magnetic photo-absorption (inverse Bremsstrahlung) [29], and a classical estimate of magnetic Compton scattering confirm the existence of these large enhancements. Further theoretical work along these lines is in progress by a Purdue-IIT-U. of Graz collaboration. The practical significance of this investigation mainly concerns the interpretation of pulsar spectra: if Compton processes are in fact important in the "magnetosphere" of pulsars, then the observed spectra will be a compound of (radiation damped) Bremsstrahlung and Compton re-scattering.

Large magnetic Compton cross-sections should be accessible to experimental measurement at NAL. Essentially this would require a change in the A beam from electron to photon bursts --- preserving the synchronization with the megagauss pulses. We would augment the MG targets with an exploding wire insert. A few microsecond pretrigger of this wire would seed the  $\gamma$ -path through the MG target with a dense ( $\sim 21 \text{ e}^-/\text{cm}^3$ ) low energy electron plasma. It would probably be most convenient to study the Compton scattering

$$\gamma + e^- + H \rightarrow \gamma + e^- + H, \quad (4.43)$$

by detecting high energy recoil electrons. We propose to carry out these studies during Phase III of the NAL experiments.

The soft photon emission associated with magnetic Bremsstrahlung is of great interest in connection with pulsar physics since it is an experimental fact that most pulsar radiation is observed in the radio frequency range ( $60 \text{ MHz} - 1100 \text{ MHz}$ ). This apparent abundance of low energy photons is quite surprising since the average photon emission energy associated with magnetic Bremsstrahlung is

$$\langle \hbar\omega \rangle \text{ (MeV)} \cong 2.05 \times 10^{-2} H(\text{MG}) E^2(\text{GeV}), \quad (4.44)$$

and one typically assigns parameter values ranging upward from  $H \sim 10 \text{ MG}$ ,  $E \sim 10 \text{ GeV}$  to the luminous portions of the pulsar "magnetospheres". We will briefly sketch an argument to show that the radio frequency tail of magnetic Bremsstrahlung is completely dominated by radiation damping phenomena [30]. Under conditions where strong vacuum polarization effects can be neglected, i.e.

$$\alpha \frac{H}{H_{\text{cr}}} \ll 1, \quad (4.45)$$

the energy levels of an electron in a uniform magnetic field are given by

$$E = mc^2 \left[ 1 + \left( \frac{P_H}{mc} \right)^2 + \frac{H}{H_{\text{cr}}} (2n + s + 1) \right]^{1/2}; \quad (4.46)$$

$$n = 0, 1, \dots; s = \pm 1;$$

where  $n$  is the principal quantum number,  $s$  denotes the spin, and  $P_H$  is the drift momentum parallel to the magnetic field direction. If the system makes a transition from an initial

("i") to a final ("f") state by the emission of a single photon, the photon energy is given by

$$\hbar\omega = \frac{mc^2}{1 - \cos^2\theta} \left\{ \left( \frac{E_i}{mc^2} - \frac{P_{Hi}}{mc} \cos \theta \right) - \left[ \left( \frac{E_i}{mc^2} - \frac{P_{Hi}}{mc} \cos \theta \right)^2 - 2 \frac{H}{H_{cr}} \Delta n_{if} (1 - \cos^2\theta) \right]^{1/2} \right\} \quad (4.47)$$

where  $\theta$  is the angle between the photon momentum and the field direction, and  $\Delta n_{if} = n_i + \frac{S_i}{2} - (n_f + \frac{S_f}{2})$ . It is easy to verify that the continuum described by (4.47) has an absolute lower bound given by

$$\frac{\hbar\omega}{mc^2} \geq \left( \frac{E_i}{mc^2} - \frac{P_{Hi}}{mc} \cos \theta \right)^{-1} \frac{H}{H_{cr}} \Delta n_{if} > \frac{1}{2} \frac{mc^2}{E_i} \frac{H}{H_{cr}}, \quad (4.48)$$

where  $E_i$ , in the last inequality, corresponds to the maximum initial electron energy. In practical units

$$\text{Min} \{ \hbar\omega \} \text{ (Hz)} = 7.15 \times 10^8 \frac{H(\text{MG})}{\text{Max} \{ E \} \text{ (GeV)}}. \quad (4.49a)$$

If one were to take this at face value, and recall that for instance pulsar NP 0532 has been observed at frequencies as low as 65 MHz [31], then (4.49a) implies that if the radiation corresponds to magnetic Bremsstrahlung, the electron energies in the magnetosphere of NP 0532 are bounded from below by

$$E(\text{GeV}) > 10 H(\text{MG}). \quad (4.49b)$$



However it is easy to see that this conclusion hinges on the neglect of radiation reaction. In case  $E \gg mc^2$ , the lifetime of an individual Landau level, is essentially independent of the energy and given by [27]

$$\tau = \frac{2\sqrt{3}}{5} \frac{\hbar}{\alpha mc^2} \frac{H_{cr}}{H}, \quad (4.50a)$$

or in practical units

$$\tau(\text{sec}) \approx 5.39 \times 10^{-12} / H(\text{MG}). \quad (4.50b)$$

Clearly this implies that the individual levels are broadened by a factor

$$\delta E \approx \frac{5\alpha}{2\sqrt{3}} mc^2 \frac{H}{H_{cr}}, \quad (4.51a)$$

or

$$\delta E(\text{Hz}) \approx 2.95 \times 10^{10} H(\text{MG}). \quad (4.51b)$$

When the level broadening becomes comparable to the level spacing, i.e.

$$\text{Min}(\hbar\omega) \approx \delta E \quad (4.52a)$$

or

$$\text{Max}\{E_i\} \gtrsim \frac{\sqrt{3}}{5\alpha} mc^2 \approx 48.5 \text{ MeV}, \quad (4.52b)$$

we encounter a condition which is analogous to the washout of ordinary cyclotron resonance in a collision dominated regime. In the present instance the collision time corresponds to the radiative lifetime. Theoretical estimates [32] and experimental observations [6] both confirm that the high energy regions of the magnetic Bremsstrahlung spectrum remain unaffected even

when (4.52a) is satisfied. This indicates that the analogy with collision damping can be taken seriously enough to serve as a model for calculations: specifically we can consider that all magnetic Bremsstrahlung in the range below (4.51b) originates from transitions between overlapping Landau levels each with a Lorentzian shape scaled by (4.50a). Preliminary results indicate that the soft photon continuum extends below the limit set by (4.49a) and that the corresponding spectral distribution is essentially independent of magnetic field strength. In view of the importance of these questions in connection with the interpretation of pulsar signals, we propose to develop extensions of the theory which will take into account the dominant influence of damping effects.

Solid state physics experiments involving magnetorefectance in the frequency range  $\sim 10^{13}$  Hz have already been carried out with megagauss targets in our Laboratory [Prof. J. Davis, private communication]. Depending on the progress of the soft photon Bremsstrahlung calculations, it may become interesting to incorporate measurements ranging downward from this spectral region in the NAL experiments.

## 5. Experimental Design Considerations

### (a) First Things First

In the SLAC experiments both the elastic and inelastic components of the magnetic Bremsstrahlung process were measured with the same set-up. Specifically the elastic component --- the deflection of electrons by a megagauss field --- was recorded on nuclear emulsions; and these emulsions simultaneously recorded

the inelastic component because the magnetic Bremsstrahlung photons were permitted to "illuminate" the plates --- the incident photons converted into pairs in the emulsions, the pair energies were determined from multiple scattering analyses, and finally the absolute flux and spectral distribution of the magnetic Bremsstrahlung were unfolded. In principle, all the information on the elastic scattering, including beam profiles, absolute flux, and other details, was available on a time scale of months. But it required over 2 years to accumulate sufficient statistics in emulsion scanning and analysis to check on the spectrum with 7% accuracy.

It is technically not advisable to attempt to duplicate this arrangement at NAL. We note for instance that the average magnetic Bremsstrahlung photon energy is given by

$$\langle \hbar\omega \rangle \text{ (MeV)} = 2.05 \times 10^{-2} H(\text{MG}) E^2(\text{GeV}). \quad (5.1)$$

The intensity decrease between  $\langle \hbar\omega \rangle$  and  $10 \times \langle \hbar\omega \rangle$ , a theoretically interesting region, is only a factor of 30, and therefore this is the preferred range for spectral measurements: at SLAC,  $H \sim 1.5 \text{ MG}$ ,  $E \sim 20 \text{ GeV}$ , and therefore we concentrated on the interval  $12 \text{ MeV} \lesssim \hbar\omega \lesssim 120 \text{ MeV}$ , which was also ideally suited for emulsion analysis of pair energies. At NAL we anticipate  $H \sim 2 \text{ MG}$ ,  $E \sim 200 \text{ GeV}$ , and the corresponding spectral range is  $1.6 \text{ GeV} \lesssim \hbar\omega \lesssim 16 \text{ GeV}$ . Existing emulsion techniques cannot distinguish pair energies of this magnitude. At SLAC we succeeded in exposing emulsions, which were positioned inside MG-targets, to the  $20 \text{ GeV } e^-$ -beam, and conceivably this technique

could be adapted to NAL. But this is problematical at best, would require a long and costly period of development, and in any case could not circumvent the n-year time scale required for emulsion analysis.

We have therefore decided in future work to split the elastic and inelastic Bremsstrahlung measurements into two phases. Although emulsions are not suitable for measuring the spectrum at NAL, a variety of possibilities involving counters and/or emulsion spectrometers are available. Unfortunately these counting systems are bound to be expensive; and therefore if we consider the two possible lines of attack:

Experiment	Principal Subsystems
$e^{\pm}$ deflection	extremely precise beam/megagauss generator/emulsions
magnetic Bremsstrahlung spectrum	precise beam/megagauss generator/counters

it is clear that Phase I should be concerned with the deflection measurement even though this imposes the most stringent requirements on the beam (see Table 1).

(b) Requirements for Phase I

As indicated previously our specific objective will be to measure the  $e^{\pm}$  deflection with sufficient accuracy to check on the characteristics of the radiation damping [cf. (4.7d)]

$$\delta\theta_{CD}(\text{mrad}) = 1.90 \times 10^{-4} H^3(\text{MG}) L^2(\text{mm}), \quad (5.2)$$

and the quantum spreading [cf. (4.41)]

$$\Delta\theta_{QM}(\text{mrad}) \approx \frac{0.95 \times 10^{-3} H^{5/2}(\text{MG}) L^{3/2}(\text{mm})}{1 + 1.33 \times 10^{-5} H^2(\text{MG}) L(\text{mm}) E_0(\text{GeV})}. \quad (5.3)$$

We must therefore make an inventory of all other effects which can give rise to a shift or spread of the beam. It is convenient to begin with the ordinary Lorentz deflection [cf. (4.7b)]

$$\theta_0 = \frac{mc^2}{E_0} \frac{H}{H_{cr}} \frac{L}{\lambda_c}. \quad (5.4)$$

The experimental error associated with the determination of  $\theta_0$  due to uncertainties in  $E$  and the path integral  $HL$  is

$$\Delta\theta_0 = - \frac{mc^2}{E_0} \frac{H}{H_{cr}} \frac{L}{\lambda_c} \frac{\Delta E_0}{E_0} + \frac{mc^2}{E_0} \frac{\Delta(HL)}{H_{cr} \lambda_c} \quad (5.5a)$$

or

$$\Delta\theta_0 \sim \theta_0 \left( \left| \frac{\Delta E_0}{E_0} \right|^2 + \left| \frac{\Delta(HL)}{HL} \right|^2 \right)^{1/2} \quad (5.5b)$$

As indicated in Table 1, we consider an uncertainty of the order of

$$\left| \frac{\Delta E_0}{E_0} \right| \sim 0.003, \quad (5.5c)$$

which was achieved during the SLAC experiments, as a reasonable design criterion for the A-beam Bremsstrahlung modifications.

The quantity  $\Delta(HL)$  is given by

$$\Delta(HL) = \left( \frac{\partial}{\partial t} \int \vec{H} \cdot \vec{d}\ell \right) \Delta t + (\text{grad} \int \vec{H} \cdot \vec{d}\ell) \cdot d\vec{r}. \quad (5.5d)$$

Analysis of the SLAC results has shown that the second term which corresponds to the spatial uncertainties can be narrowed down by

combining the following techniques: (i) direct measurement of the MG fields with small inductive probes; (ii) flash X-ray records of the MG targets at the time of the high energy beam pulse; and (iii) detailed field profile measurements in enlarged mock-up coils, where the skin depth is appropriately scaled by adjusting the frequency of the generator that feeds the coils. The net spatial uncertainty can be cut down to 1% by these means. The limiting factor is the accuracy of the MG-probe calibration. If differential methods, such as the relative  $\pi^{\pm}$ ,  $e^{\pm}$  magnetic deflection outlined in (4.8)  $\rightarrow$  (4.10c), were utilized the absolute field calibration could of course be avoided.

The first term in (5.5d) corresponds to the temporal uncertainties which are associated with the field variation and the target expansion. From the SLAC results we know that  $|\dot{H}| < 0.2 \text{ MG}/\mu\text{sec}$  during an  $0.3 \mu\text{sec}$  interval centered on the field peak. Furthermore it has been found that tantalum targets run at 2 MG distent with velocities less than  $0.07 \text{ mm}/\mu\text{sec}$  [5]. Therefore during an  $0.1 \mu\text{sec}$  beam pulse the temporal uncertainties are at most 1%.

Finally combining (5.5b, c, and d) we estimate that the total uncertainty and/or smearing in the deflection is given by

$$\Delta\theta_0 \sim 0.015 \theta_0.$$

Comparing with Table 3, it is clear that for  $H \gtrsim 2 \text{ MG}$ ,  $L \sim 10 \text{ mm}$ , we obtain a signal/noise ratio  $\gtrsim 4$ .

Beam shifts and beam spreads can also be caused by: (i) field inhomogeneities; (ii) transverse field components; (iii)

induced electric fields; and (iv) misalignment (or divergence) of the beam and the MG-target fields. These problems have already been discussed in Section 4b. In particular the sequence of estimates (4.30b  $\rightarrow$  e) shows that these perturbations have a negligible influence. Once the beam characteristics and final MG-field configurations are known, we expect to recheck these calculations with detailed computer simulations.

The most stringent beam parameter constraint indicated on Table 1 is the horizontal beam divergence  $\Delta \theta_{\text{Div}}^{\text{horiz}} \sim 0.03$  mrad. Comparison with Table 3 makes it clear that this corresponds to

$$\delta \theta_{\text{CD}} \approx \Delta \theta_{\text{QM}} \approx 4 \Delta \theta_{\text{Div}}^{\text{horiz}}, \quad (5.6)$$

for  $H \gtrsim 2$  MG,  $L \sim 10$  mm. In view of the quality of the SLAC data, we consider this a conservative signal to noise ratio.

Next we note that the radiation reaction shifts and quantum broadening should exceed the beam divergence produced by the multiple scattering of electrons between the final beam defining elements, the MG-targets, and the detection system. The multiple scattering divergence is of the order of

$$\Delta \theta_{\text{MS}} (\text{mrad}) \sim \frac{21 \ell_{\text{RL}}^{1/2}}{E(\text{GeV})}, \quad (5.7)$$

where  $\ell_{\text{RL}}$  is the interposed thickness of material measured in radiation lengths. If we make the (only reasonable) choice

$$\Delta \theta_{\text{MS}} \approx \Delta \theta_{\text{Div}}^{\text{horiz}} \lesssim 0.03 \text{ mrad}, \quad (5.8)$$

it's trivial to invert (5.7) in order to obtain estimates for

the maximum tolerable beam obscuration. Some representative values are given in Table 4.

Table 4. Upper Limits on Multiple Scattering  
 $[\Delta\theta_{MS} \lesssim 0.03 \text{ mrad}]$

Energy	Air	Mylar	Aluminum	Tantalum	Emulsion
150 GeV	1390 cm	520 mils	161 mils	5.4 mils	1340 $\mu$
300 GeV	5560 cm	2080 mils	643 mils	21.6 mils	5360 $\mu$

This table suggests the following conclusions:

- (1) Insulation against flash-over in the MG-targets will not be a problem since 2.5 mils mylar is adequate to stand off 20 kV.
- (2) If it turns out to be technically advantageous to incorporate the dielectric switch --- a 10 mil mylar, 5 mil aluminum sandwich --- in the MG-target loop, beam degradation will not be a limiting factor.
- (3) The entire experiment, beyond the last beam defining element, can be set up without vacuum.

#### (c) Beam Intensity and Emulsion Detectors

In the previous sub-section we have shown that the stringent beam requirement for phase I, i.e.  $\Delta\theta_{Div}^{horiz} \lesssim 0.03 \text{ mrad}$ , is an ineluctable consequence of the parameter ranges associated with the NAL accelerator and our megagauss generators. In the present section we will show that this unusual requirement is rendered practicable by another unusual feature, namely that very low beam intensities ( $10^2 - 10^3 \text{ e}^-/\text{pulse}$ ) turn out to be optimal for the emulsion detectors. Let us consider the worst possible



case: This corresponds to an axially symmetric sharpening of the A-beam spot size and divergence angle as indicated on Table 1. If this is accomplished solely by tighter collimation, the corresponding reduction in beam intensity is given by

$$I_{Br} \gtrsim (\text{Ratio of Beam Areas at Target}) \times (\text{Ratio of Divergence Angles})^2 I_A, \quad (5.9a)$$

where "A" denotes the A-beam, and "Br" the modified beam for the Bremsstrahlung experiment (Phase I). Inserting values from [10] and Table 1, we find:

$$I_{Br} \gtrsim \frac{1 \text{ mm} \times 1.5 \text{ mm}}{13.2 \text{ mm} \times 8.1 \text{ mm}} \left( \frac{0.03}{0.3} \right)^2 I_A, \quad (5.9b)$$

$$\gtrsim 1.4 \times 10^{-4} I_A.$$

In view of the fact that  $I_A \sim 10^7 - 10^8 \text{ e}^-/\text{pulse}(20 \mu\text{sec extraction})$ , (5.9b) indicates that  $I_{Br}$  will fall in the range  $10^3 - 10^4 \text{ e}^-/\text{pulse}$ . There are two further compensating factors that have to be taken into account: (1)  $I_{Br}$  will be reduced from this nominal estimate by a factor of 30 - 200 because the Bremsstrahlung pulses will be shortened to  $0.1 \mu\text{sec}$  and this will result in an intensity loss proportional to the ratio  $(0.1 \mu\text{sec}/\text{accelerator fast extraction time } [\sim 20 \mu\text{sec}])$ . (2) The estimate (5.9b) is too pessimistic since Table 1 and (4.30d) indicate that a vertical divergence of  $\Delta\theta_{Div}^{vert} \sim 0.3 \text{ mrad}$  is acceptable, and furthermore some of the  $A \rightarrow B_r$  beam modifications can be implemented with improved focussing which will not squander so much intensity. This should

yield an increase by at least a factor of 20. Finally, combining the worst possible contingencies implied by (1) and (2), we can rewrite (5.9b) as

$$I_{Br} > \frac{20}{200} \times 1.4 \times 10^{-4} I_A$$

$$> 1.4 \times 10^{-5} (10^7 - 10^8) \sim 140 - 1400 \text{ e}^- / 0.1 \mu\text{sec.} \quad (5.9c)$$

This intensity range is ideally matched to the requirements of the emulsion detection system. It is known on the basis of the SLAC experiments that a 1 mm diameter beam is nearly optimal for the MG-targets. If for the moment we neglect beam divergence, this corresponds to a  $(\pi/4) \text{ mm}^2$  illuminated spot on the emulsions. Since  $50\mu \times 50\mu = 1$  field of view (fv) under normal scanning conditions, we have  $(\pi/4) \text{ mm}^2 \Leftrightarrow 314 \text{ fv}$ . An experimentally reasonable and efficient lower limit for locating high energy electron tracks in emulsion is 1 track per 3 fv; this implies a minimum beam intensity of 100  $\text{e}^-$  per  $0.8 \text{ mm}^2$  beam burst. This is of course compatible with the lowest bound given in (5.9c). For completeness sake we note that  $5 \times 10^6 \text{ e}^-$  is an upper bound for the number of tracks that can be distinguished. The visual threshold is approximately at  $10^3 \text{ e}^-$  per  $\text{mm}^2$ .

The actual measurement of (5.2) and (5.3) can be carried out by two principal methods:

- (1) Simple Deflection - Suppose that a single emulsion plate were located at a distance D downstream from the MG-target and oriented transverse to the beam direction. Then the ordinary Lorentz deflection (4.7b) corresponds to a lateral displacement of

$$S(\text{mm}) = 29.98 D(\text{m}) H(\text{MG}) L(\text{mm})/E(\text{GeV}), \quad (5.10)$$

on the emulsion. The radiation reaction shift (5.2) would increase  $S$  by an increment

$$\delta S_{\text{CD}}(\text{mm}) = 1.90 \times 10^{-4} D(\text{m}) H^3(\text{MG}) L^2(\text{mm}). \quad (5.11)$$

Let us consider the specific case  $E \sim 150$  GeV,  $H \sim 2$  MG,  $L \sim 10$  mm. In view of Table 4, it is plausible that  $D \sim 1$  m, is a practical choice for the emulsion placement. Then  $S \sim 4$  mm, and  $\delta S_{\text{CD}} \sim 0.15$  mm. Suppose for the moment we ignore (5.3), but take into account  $\Delta \theta_{\text{Div}}^{\text{horiz}} \sim 0.03$  mrad, and assume that at the MG-target the beam diameter is 1 mm. In principle then the deflected beam corresponds to a spot of  $(1 + 0.06)$  mm diameter on the emulsion, which is displaced by a distance of  $(4 + 0.15)$  mm from the forward direction. The forward direction --- as in the SLAC set-up --- is defined by surveying and a fiducial (= "target empty") beam pulse. In practice therefore we must measure the distance between two spots, each 1 mm in diameter, separated by 4 mm, to better than 0.1 mm precision. This is essentially a problem in geometrical probability since each "spot" actually consists of an aggregate of  $N$  ( $\sim 100$ )  $e^-$  tracks dispersed over an area of  $0.8 \text{ mm}^2$ . The position of each track can be determined to better than  $2\mu$  by standard scanning methods. If only one track were available the uncertainty in the location of the center of the spot would be 0.5 mm. By straightforward statistical methods one can then show that the uncertainty corresponding to  $N$  tracks is  $0.5 N^{-1/2} < 0.05$  mm

for  $N \geq 100$ . The required precision and statistics are therefore well coordinated with the beam intensity estimates (5.9c).

This experimental procedure is not suitable for detecting the quantum spread (5.3); and even with regard to the radiation reaction shift (5.2) should be considered only as a useful preliminary in checking out the  $A \rightarrow Br$  beam modifications. We propose to carry out the definitive Phase I measurements with an

- (2) Emulsion Goniometer - In principle a direct measurement of the angles (and angular distributions) corresponding to (5.2) and (5.3) could be carried out with a single thick emulsion. If this were placed  $\sim 12$  cm downstream from the MG-target and exposed to both a fiducial pulse and a pulse deflected by the MG-field, then there would be a  $\sim 0.5$  mm lateral interval in which electron tracks from both pulses would be mingled in the emulsion. Specifically, in the scattering plane we would see two groups of tracks, one colinear to  $\pm 0.03$  mrad, and the other colinear to  $\pm 0.1$  mrad, with the overall property that these two groups would have a mean divergence angle of 4 mrad. In practice this would be difficult to implement because of the distortions which arise in developing  $\sim 600 \mu$  emulsion, and also because of the limited precision ( $\sim 1$  mrad) of the measurements of the track directions. Of course this could be sharpened by a factor of 10 by using statistics, but then there would be no essential improvement over Method 1.

In order to exploit the superior spatial resolution of emulsions for goniometric purposes it is essential to use at least two thin ( $\sim 25 \mu$ ) emulsions separated by, say,  $10 \text{ cm} = 10^5 \mu$ . If these emulsions are placed 50 cm and 60 cm downstream from the MG-targets, then the deflected beam would leave two successive spots, each a millimeter in diameter, and displaced by 2.0 mm and 2.4 mm respectively from the forward direction. In order to key the emulsions together precisely, and to establish their orientation with respect to the "forward" direction, we now translate both emulsions rigidly by 2 mm in a direction transverse to the beam, and register a fiducial pulse. Since the emulsions are thin, distortion will be negligible. Crude alignment of the two emulsions ( $\sim 20 \mu$ ) can be secured by commercial micropositioning film plate holder assemblies of the type used in holographic interferometry. The final alignment can be made under the scanning microscope by matching the tracks of the fiducial pulse electrons. The angular distribution of the deflected electrons can then be inferred from the lateral offset of their tracks in the two emulsions. The resolution of this method is clearly  $2 \mu / 10^5 \mu \sim 0.02 \text{ mrad} \sim 4 \text{ sec of arc}$ .

The emulsion positioning and alignment can easily be accomplished with commercially available interferometric equipment. The essential requirement is the rigid translation of the emulsion assembly. Commercial stages with straight runs accurate to  $\pm 1 \mu$  per 100 mm translation are also available for this purpose. The only novel feature of the set-up will be the remote control of the positioning devices. This is desirable in order

to speed up the experiment and to reduce the background radiation exposure levels for emulsions and humans. This technique was already used for the MG-target positioning at SLAC.

## 6. Plan of the Complete Experiment

In this Section we shall outline the equipment requirements and the preparatory experimental developments for the Phase I NAL Bremsstrahlung experiment. The operating sequence for all stages requiring a set-up at NAL and beam time are discussed in Section 7. In order to make the Budget [Section 9] more intelligible, estimates for all principal new items of equipment and fabrication costs are listed in each of the following sub-sections.

### (a) Condenser Bank

The operating characteristics of the bank we have available at present are as follows:

Total Energy	60 kJ
Voltage	20 kV
Peak Current	2 MA
Inductance	12 nH
Resistance	6 m $\Omega$
Quarter Period	2 $\mu$ sec
Switching Time	1 $\mu$ sec
Switch Jitter	$\sim$ 50 nsec

In order to adapt the bank for the NAL experiments a number of modifications will be made:

- (1) Dielectric Switch Pulser - At present the bank is actuated by rupturing a dielectric switch with exploding wires. The pulsing unit is a homemade, 4J, 4 kV amplifier which is

discharged through a Krytron KN6B tube. The total time jitter of this system is  $\sim 50$  ns. The overall performance of the KN6B's is not satisfactory. It is advisable to upgrade this unit to give more reliable, low jitter switching. There are two possibilities: SLAC is willing to make available a two stage thyatron pulser (F103 & CH 111) which can deliver 13.5 J at 7.5 kV; the total system delay is  $\sim 250$  ns and the jitter is  $\sim 3$  ns. The estimated cost is \$6,000. The Field Emission Corp. could provide a low jitter thyatron amplifier (1563 + 1027) driving a Marx generator (2722 - two modules); this system would deliver 12 J at 60 kV with an overall delay of 200 nsec and a jitter of less than 5 nsec. The cost is \$5,000. In principle, both systems would provide the desired improvement in low jitter performance and higher energy pulses. The final choice will depend on the design of 2 pulse (and voltage isolation) transformers to match these pulsers to the load. Depending on the type of dielectric switch (see below) the load can be either high or low impedance. The design and fabrication of these transformers will cost  $\sim \$450$ .

- (2) Dielectric Switch - Some of the present switch inductance can be traced to the use of exploding wires. We plan to explore two modifications: The most obvious improvement is to retain the present collector plate-switch arrangement, but to change from exploding wires to a tetrode configuration of mylar and aluminum strips [8]. This should facilitate low jitter performance, and spread the current over the

whole width of the strip; pinch spots which constitute high inductance bottlenecks are thereby avoided. The other possibility for improvement is more radical: We would like to try combining the dielectric switch with the MG-coil. This has the advantage of consolidating all the self-destructing elements in one unit, and ameliorates the inductance problem by switching at the unique location where all the current is concentrated anyway. Both of these options will require some development and testing before a final decision for NAL can be made.

- (3) Relocation and Enlargement - The condenser bank and all other major equipment utilized in the megagauss research program is presently located in the basement of an old building. Our power requirements far exceed the available electrical circuits; safety is a continuing problem; and the steady deterioration of the facilities has made staff retention difficult. These problems have been brought to the attention of the IIT Administration and we have secured their commitment to support the NAL-megagauss experiments by relocating the Magnet Laboratory in modern facilities. Specifically Rooms 215, 216, and 219 of Siegel Hall (Physics Building) will be consolidated with a large corridor and remodeled to provide about 2,000 ft<sup>2</sup> of air conditioned laboratory space. About 30 kW of stabilized power will also be available. In the budget we are requesting \$12,000 to help defray special costs associated with the installation of safety blast shielding for the bank, a venting system, and electrical and control cabling.



The energy storage capacitors currently in service are Sangamo #740503 ( $14 \mu\text{F}$ , 20 kV, 50 nH). In order to enlarge the bank from 60 to 80 kJ, lower the inductance, simplify and strengthen cable connections to the capacitors, and provide spares for ageing units, we are requesting 30 new Sangamo #740515 ( $14 \mu\text{F}$ , 20 kV, 15 nH) capacitors; total cost \$10,800.

(b) MG-Target Design

Most of the SLAC experiments were carried out with copper coils. These distended with velocities of  $\sim 1 \text{ mm}/\mu\text{sec}$  at the 2 MG level. The time scale of this deformation is essentially governed by the Alfvén velocity which is proportional to  $H\rho^{-1/2}$ , where  $\rho$  is the density of the material. Prompted by this observation we carried out a series of tests with tantalum coils and obtained striking improvements in the coil stability. Flash X-ray checks showed that at 2 MG, the expansion velocities were less than  $0.1 \text{ mm}/\mu\text{sec}$ . We are of course not sure that tantalum is the optimum material; "heavimet" is another promising high density candidate with favorable conductivity characteristics. Clearly a series of tests is necessary to identify the best coil material.

The SLAC configuration can also be improved by reshaping the targets so as to maximize  $\int \vec{H} \cdot d\vec{\ell}$  along the beam trajectory. The cylindrical design of the SLAC coils was convenient and cheap from the standpoint of fabrication, but was extremely wasteful in generating megagauss fields where they were not needed. We propose to investigate coil designs which approximate miniaturized

parallel plate transmission lines. These approach the ideal of maximum  $\int \vec{H} \cdot d\vec{\ell}$  for a given bank energy, and have the elegant feature that the open end of the line serves as a beam hole. If tests confirm that this is a practicable target design, the bank termination can easily be modified to allow longitudinal passage of the  $e^-$ -beam.

The estimated fabrication costs for the coil assemblies ( $\sim 50$ ), bank termination, and collector plate are \$6,500. The coil deformation studies would be facilitated by a second flash X-ray channel; this would require only two add-on modules for our present FX-2722 system (1563/1027, cost of new components \$4,840).

#### (c) Instrumentation

Practically all the electronic instruments necessary for the NAL experiments are available in the Magnet Laboratory. Our 9 Tektronix 556 scopes have seen hard use since 1968, and need re-alignment; the total cost for a factory overhaul is \$1,100. When the Magnet Laboratory is relocated in Siegel Hall, it will be necessary to shield the oscilloscopes from the bank. A wire screen Faraday cage will be built around the bank; the oscilloscopes should be mounted in a fully shielded room, e.g. Lindgren #34 (\$4,000).

The master timing sequence for the NAL experiments will be initiated by a pre-pulse from the accelerator control system. The trigger logic will determine the functioning of the beam stoppers, MG bank discharge, flash X-ray, and 18 scope channels. This sequence is usually derived from a digital delay generator.

Our Rutherford A-10 is inadequate since only 3 delay channels are available and the timing accuracy is limited to  $0.1 \mu\text{sec}$ . A Cordin 432 digital delay generator (\$5,600) will provide the required precision and flexibility.

(d) Emulsion Goniometer

The electron tracks will be recorded on Ilford G-5 and/or K-5 emulsion. Since these plates will be thin ( $\sim 25 \mu$ ), we can probably process them locally and do some preliminary scanning at NAL (or IIT). The final measurements and analysis will be carried out at Dr. Heckman's emulsion laboratory at Berkeley. The emulsion holders for SLAC were custom made and expensive. It will probably be more economical to build the NAL goniometer with commercial units, e.g. NRC plate holders (#800, cost \$275 each).

There are two principal reasons for providing a remote positioning capability for the goniometer assembly: (1) As indicated in Section 5(c), it is desirable to rigidly translate the emulsions by 2-3 mm between the MG-shot and the registration of the fiducial pulse. The angular rotation of the assembly during this translation must not exceed 4 sec of arc. (2) Although in principle only two pulses are necessary to define the  $e^-$  deflection angles, the vagaries of accelerator operation will sometimes require extra pulses. The analysis and interpretation of some of the plates exposed at SLAC were confused by the background caused by these extra "inspection" pulses. Since experience has shown that opening up the target area to personnel for the re-adjustment of plates is too time consuming, we plan to house the NAL emulsion goniometer in a small cave where it will be shielded

against low energy background, and to position it automatically for the MG and fiducial pulses. If beam re-tuning is necessary during a run, the emulsions could be remotely taken out of the beam and protected in the cave.

All of this manipulation can be conveniently taken care of by adapting the MG-target positioning equipment left over from the SLAC experiment. This consists of a mill base which is actuated by servo-motors. This type of combination is standard in the numerically controlled machine tool industry. Adjustments down to 0.001" in absolute position can easily be made. The shielding cave will be a lead brick housing, with moveable door, built around one end of the mill table. The goniometer assembly can quickly be run out of the cave and positioned for the MG and fiducial pulses. The only expense involved is moving the equipment to NAL and replacing the present feed with a more accurate ball screw feed (cost \$1,800).

#### 7. The Bremsstrahlung Experiment at NAL

The major problem in fitting the Bremsstrahlung experiment into the overall research schedule at NAL will be to find a location where most of the time there is no beam, and which is sufficiently remote, in an electrical sense, so that the repeated discharges of the 80 kJ bank will not impair the operation of other experiments. The final set-up at SLAC is shown on the appended blueprint. The grouping of equipment will be approximately the same at NAL. The specific experimental modules are as follows:

## (a) Listing of Experimental Modules

(1) Target and Bank Module

condenser bank	megagauss target
charging and switching circuits	beam alignment jigs
flash X-ray heads	mill base and NC circuits
thyratron pulser	field sensors
dielectric switch	

(2) Detector Module

emulsion goniometer	mill base and NC circuits
shielding cave	X-ray film
	beam defining counters

(3) Control Module

(a) condenser bank charging supply

flash X-ray controls

remote NC controls for MG-target and emulsions

(b) In Screened Room

timing circuits

oscilloscopes (18 channels)

counter displays

(4) Beam (Special Elements for  $A \rightarrow Br$  Conversion)

stopper	} plunger	collimators
counter		operated counter (downstream from emulsions)
special pulsed magnets		

As indicated previously, the MG-target positioning techniques utilized at SLAC worked so well that we are planning to adapt them to the shielding and manipulation of the emulsion goniometer. This means that a second mill base and associated NC controls

will have to be acquired for the MG-target. The estimated cost for this equipment is \$18,000.

(b) Construction of Modified A-Beam

At SLAC a new electron beam line (9') was installed to meet the particular requirements of the magnetic Bremsstrahlung experiment. This beam is described in detail in reference [9]. Although the problems involved in deriving an appropriate beam from the NAL machine are entirely different, we have previously indicated that the proposed  $e^-$  A-beam design already comes close to our requirements. The specific beam characteristics are described in Table 1. We expect that Dr. D. White will be granted permission to collaborate with the NAL beam design staff to work out the optimum solution for modifying the A-beam. This will involve the installation of additional collimators, special pulsed magnets, fast stopper, a removable counter, and probably at least one focusing element (quadrupole ?). Due to the electrical "noise" associated with the condenser bank it will probably be advisable to place the Bremsstrahlung experiment behind all the other set-ups in the A-line, or to construct a side-stub.

The IIT-Purdue group can provide (i) the theoretical design assistance, (ii) the collimators; (iii) fast stopper; and (iv) removable counter. We also expect to provide the special pulsed magnets in cooperation with SLAC and NAL.

At SLAC the beam defining instrumentation in the 9' line was limited to 2 scintillation counters and an ion chamber. These were all installed downstream from the emulsion stand. At NAL we would like to make two essential improvements: (1) A removable

beam inspection counter should be installed upstream from the fast stopper. Due to the extraordinarily low intensity of the operating beam ( $\sim 10^3 e^-$ ) this counter will probably have to include a showering element, or be operated in conjunction with a removable attenuator (= scattering diaphragm). (2) It would be highly desirable to have an independent check of the length of the pulse that is deflected by the MG-target. At SLAC this information was derived from one of the scintillation counters. Unfortunately noise from the condenser bank discharge partially obscured these signals. We hope that at NAL it will be possible to allocate sufficient space so that the beam run downstream from the MG-target can extend circa 60'. Shielded counters installed at this distance should be essentially invulnerable to noise from the bank. Furthermore, this maneuverability in space will be essential when we install the counters for Phase II.

#### (c) Beam Time Requirements

Based on our experience at SLAC, one can estimate reliably that Phase I can be completed with 20 full scale shots, including tune-up trials. The intrinsic time scale of the experiment is of course 100 nsec. The time between shots, allowing for refurbishing of the dielectric switch, MG-target mounting and alignment, and replacement of the emulsions, is one hour. At SLAC, the overriding time requirement was the switching and tuning of the beam; this frequently took 4 hours. We expect that careful design of the A-beam modifications for the Bremsstrahlung experiment will reduce the corresponding switch-over time at NAL to more acceptable levels.

We expect that it will take roughly 12-18 months to carry through the A-beam modifications and to prepare the experimental area for the Bremsstrahlung experiment. This is approximately the same time period that will be required for relocating the Magnet Laboratory at IIT, and upgrading the bank, target, and instrumentation in accordance with the specifications outlined in this proposal.

The referees may be interested to note that in the original SLAC proposal (submitted in December 1968) we estimated that it would take 12 months to run the first complete Bremsstrahlung experiment. The actual time scale was: 1 July 1969 - grant begins; 4 August 1970 - first complete Bremsstrahlung experiment. We are confident that we can sustain an equally vigorous pace of development in carrying out the NAL experiments. The fact that we will be participating in the creation of the electron-photon facilities at NAL should be of general benefit to the laboratory and contribute to the success of the Bremsstrahlung experiments.

#### 8(a). References

- [1] C. S. Shen, Phys. Rev. Lett. 24, No. 8, 410-15 (23 Feb. 1970).
- [2] H. G. Latal, Acta Phys. Austriaca 34, 65-82 (1971).
- [3] C. S. Shen and D. White, Phys. Rev. Lett. 28, No. 7, 455-59 (14 Feb. 1972).
- [4] D. White, PhD Dissertation, Purdue, 1972 (unpublished).
- [5] R. C. McBroom, MS Dissertation, IIT, 1971 (unpublished).
- [6] M. Mashkour, PhD Dissertation, IIT, 1972 (unpublished).
- [7] T. Erber, F. Herlach, M. Mashkour, R. C. McBroom, H. Heckman, J. J. Murray, R. Gearhart, (in preparation).



- [8] A. R. Miller, DASA 2260, MLR 11 (1969); and private communication.
- [9] F. Herlach et al. , Proc. IEEE Trans. Nucl.Sci. NS-18, No. 13, 809-14 (June 1971).
- [10] T. Nash, TM-371/6020 (May 1972); A. L. Read, PAC-Photon Workshop Document (May 1972).
- [11] T. Erber, Fortschr. Phys. 9, 343-92 (1961).
- [12] C. S. Shen, Phys. Rev. D 6 No. 10, 2736-2754 (1972).
- [13] T. Erber, Schladming Lectures, Acta Phys. Austriaca, Suppl. VIII, Springer, Wien, 1971; pp. 323-57.
- [14] R. F. O'Connell, "Physics of Dense Matter," IAU Symposium, Boulder, Aug. 1972.
- [15] P. Goldreich and W. Julian, Astr. Jr. 157, 869 (1969).
- [16] V. Canuto and H. Y. Chiu, Space Sci. Rev. 12, 3-74 (1971).
- [17] F. Herlach, D. Kachilla, and T. Erber, Rev. Sci. Instr. 41, 1-7 (1970).
- [18] E. C. Cnare, private communication.
- [19] T. Erber, Rev. Mod. Phys. 38, 626-59 (1966).
- [20] F. Rohrlich, "Classical Charged Particles," Addison-Wesley, 1965.
- [21] T. C. Mo and C. H. Papas, Phys. Rev. D4, No. 12, 3566-71 (1971).
- [22] G. Bathow, E. Freytag, and R. Haensel, Jr. Appl. Phys. 37, 3449-54 (1966).
- [23] J. K. Hale and A. P. Stokes, Jr. Math. Phys. 3, 70 (1962).
- [24] G. N. Plass, Rev. Mod. Phys. 33, 37-62 (1961).
- [25] H. Arzeliès, "Rayonnement et Dynamique du Corpuscule Chargé Fortement Accéléré," Gauthier-Villars, Paris, 1966.

- [26] L. I. Schiff, Am. Jr. Phys. 20, 474 (1952).
- [27] A. A. Sokolov and I. M. Ternov, "Synchrotron Radiation," Pergamon, 1968.
- [28] P. Urban and K. Wittmann, Acta Phys. Austriaca, 36 18-26, (1972).
- [29] P. Urban and K. Wittman, Acta Phys. Austriaca, 35, 9-31 (1972).
- [30] T. Erber and H. N. Spector (submitted for publication).
- [31] J. M. Rankin et al., Astroph. Jr. 162, 707-725 (1970).
- [32] D. White, Phys. Rev. D 6, 2080-85 (1972).

#### 8(b). Figures

1. The range of validity of different theoretical descriptions of magnetic Bremsstrahlung [12]:

Region 1 - classical electrodynamics; negligible radiation reaction.

Region 2 - classical electrodynamics; strong radiation reaction.

Region 3 - quantum electrodynamics; weak radiative corrections (see however [30]).

Region 4 - quantum electrodynamics; strong radiative corrections.

Region 5 - non-perturbative regime of QED; fields larger than  $H_{cr}$ .

The regions a,...,e correspond to the following situations:

a - cosmic ray electrons in galaxy.

b - relativistic electrons in crab nebula.

c - electron synchrotrons.

d - megagauss Bremsstrahlung (SLAC).

e - megagauss Bremsstrahlung (NAL).

The shadowed rectangle corresponds to pulsar electrodynamics.

2. Computer simulation of quantum straggling effects:  
 $E_0 = 100 \text{ GeV}$ ,  $H = 3 \text{ MG}$ ,  $L = 5 \text{ mm}$ .
3. Computer simulation of quantum straggling effects:  
 $E_0 = 500 \text{ GeV}$ ,  $H = 1 \text{ MG}$ ,  $L = 5 \text{ mm}$ .
4. Computer simulation of quantum straggling effects:  
 $E_0 = 100 \text{ GeV}$ ,  $H = 7 \text{ MG}$ ,  $L = 5 \text{ mm}$ .
5. Schematic of beam deflection by MG-target:  $\theta_0$  corresponds to the ordinary Lorentz deflection;  $\delta\theta$  is the additional deflection due to radiation reaction; and  $\Delta\theta$  indicates the quantum straggling.
6. Schematic of the emulsion set-up at SLAC [6].
7. Magnetic Bremsstrahlung spectrum determined by emulsion measurements:  $E = 19 \text{ GeV}$ ,  $H = 1.6 \text{ MG}$  [6].
8. Appended: Layout of Bremsstrahlung experiment at SLAC.
9. Appended: Proposed Layout of beam and experiment at NAL.

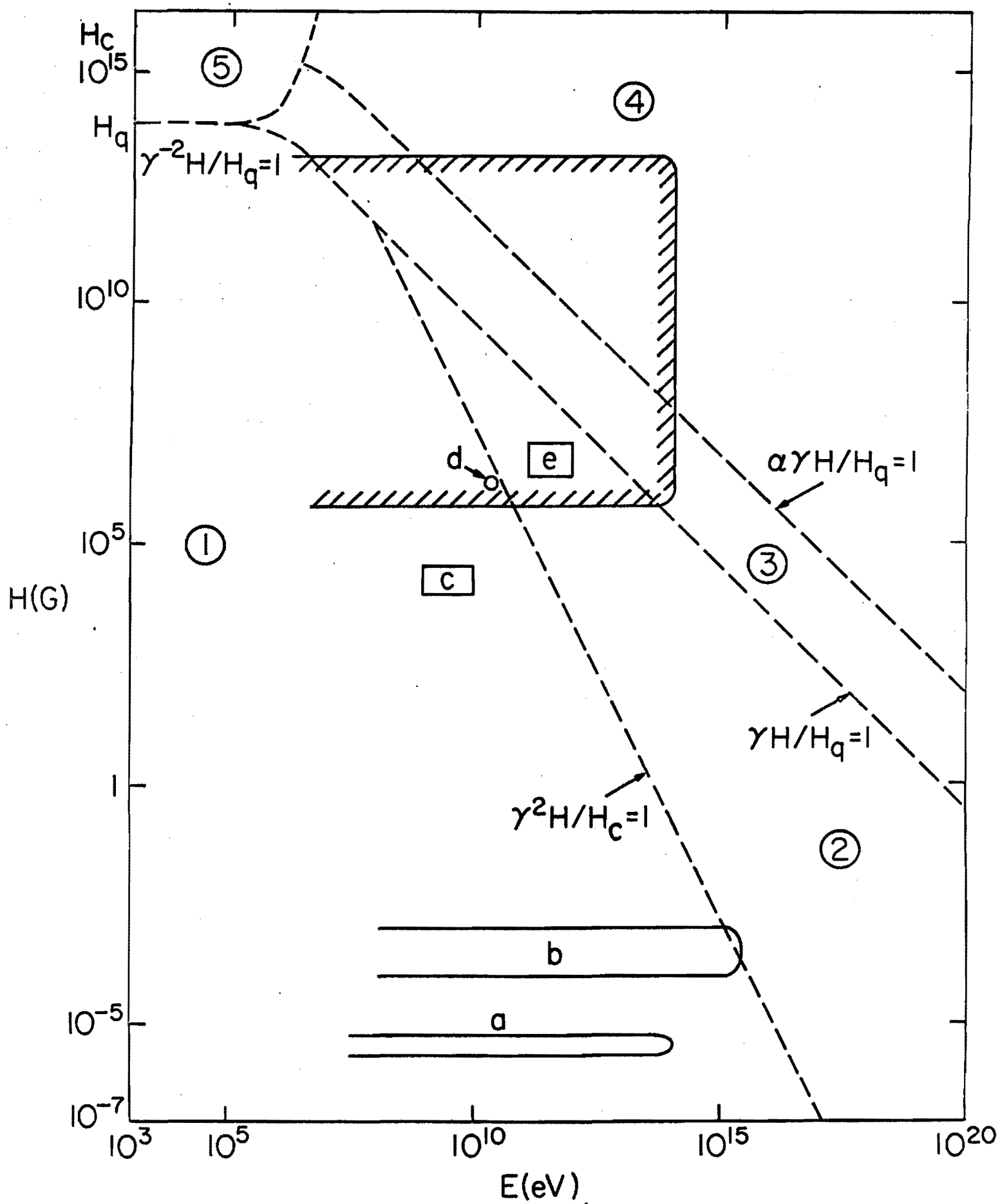


Fig. 1

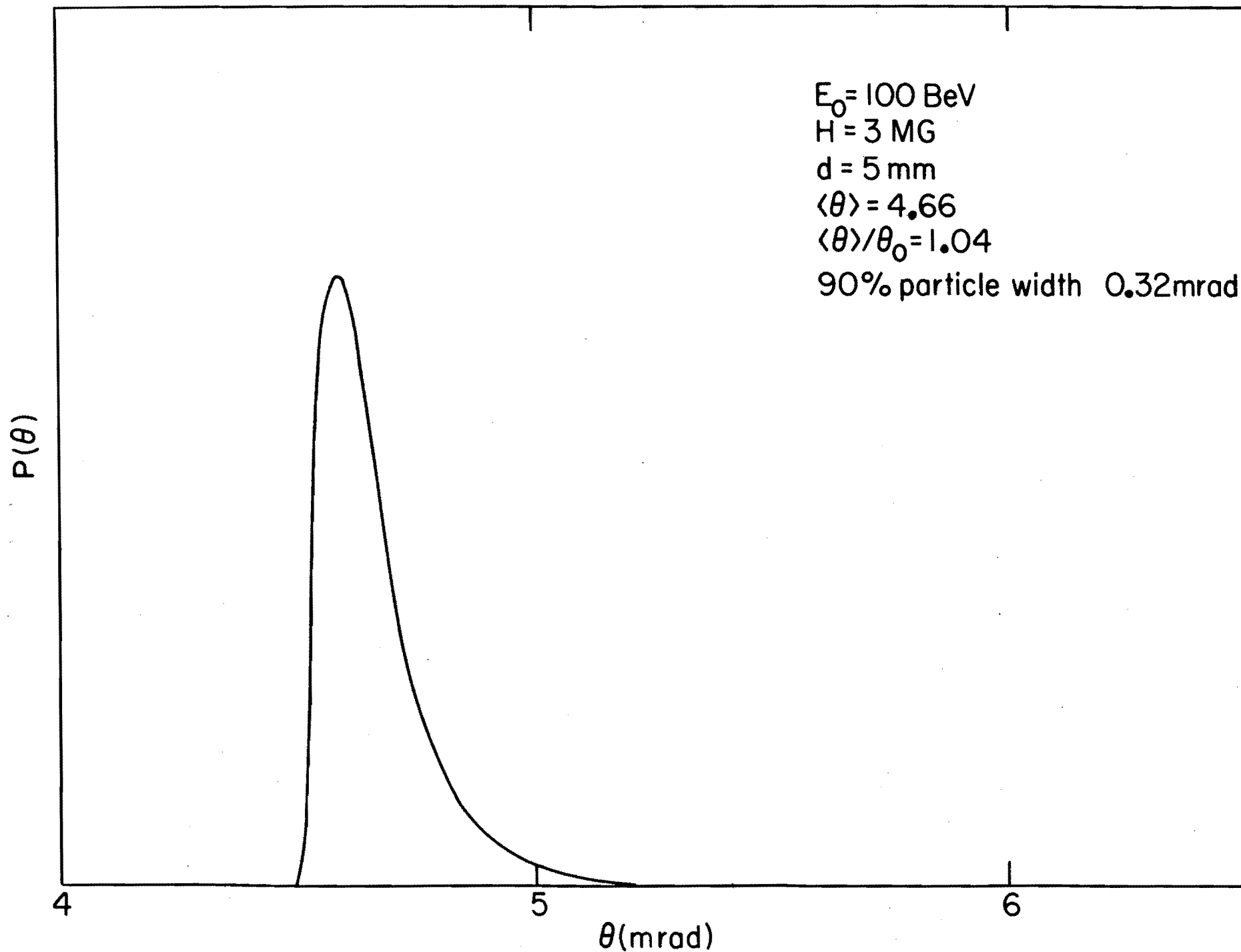


Fig. 2

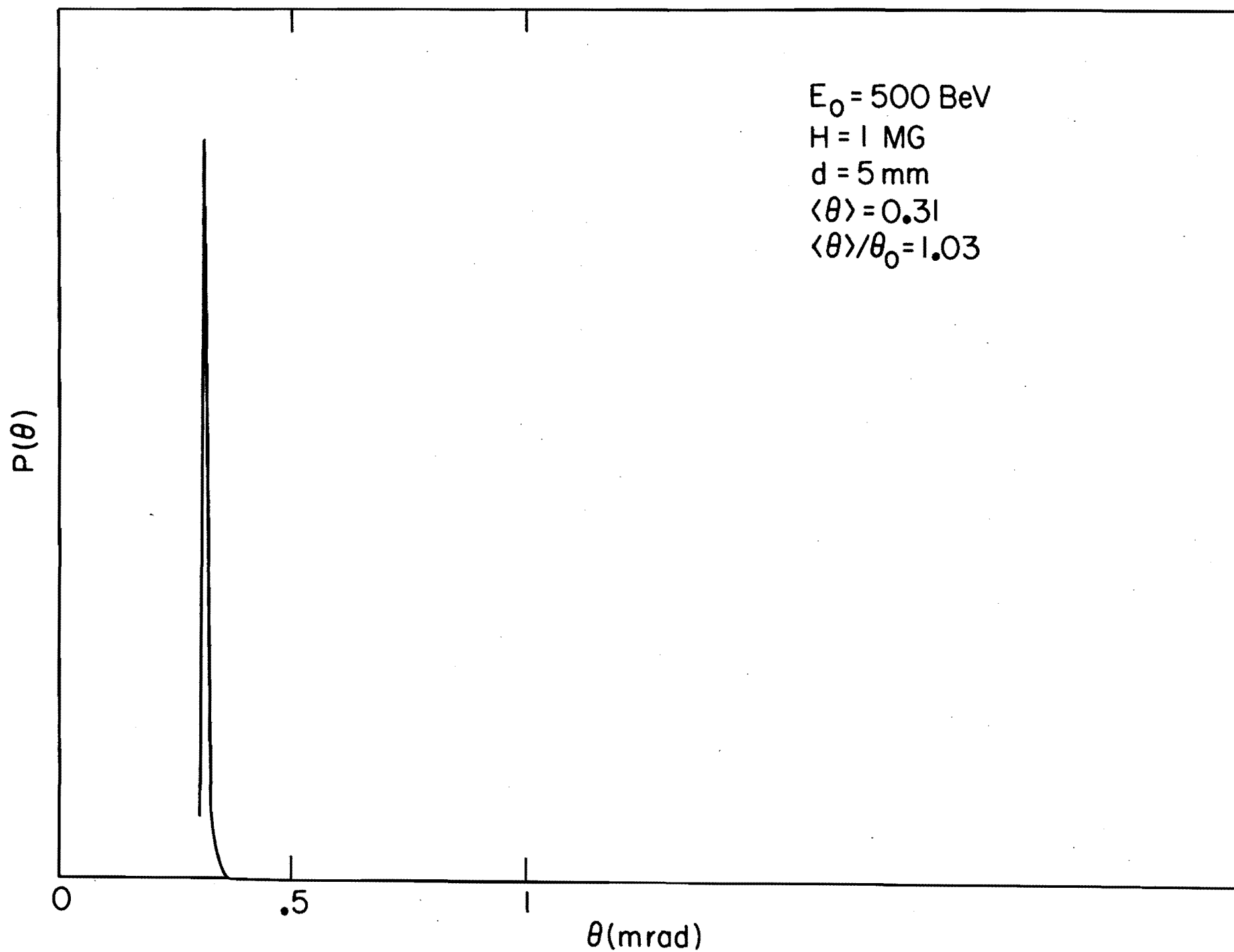


Fig. 3

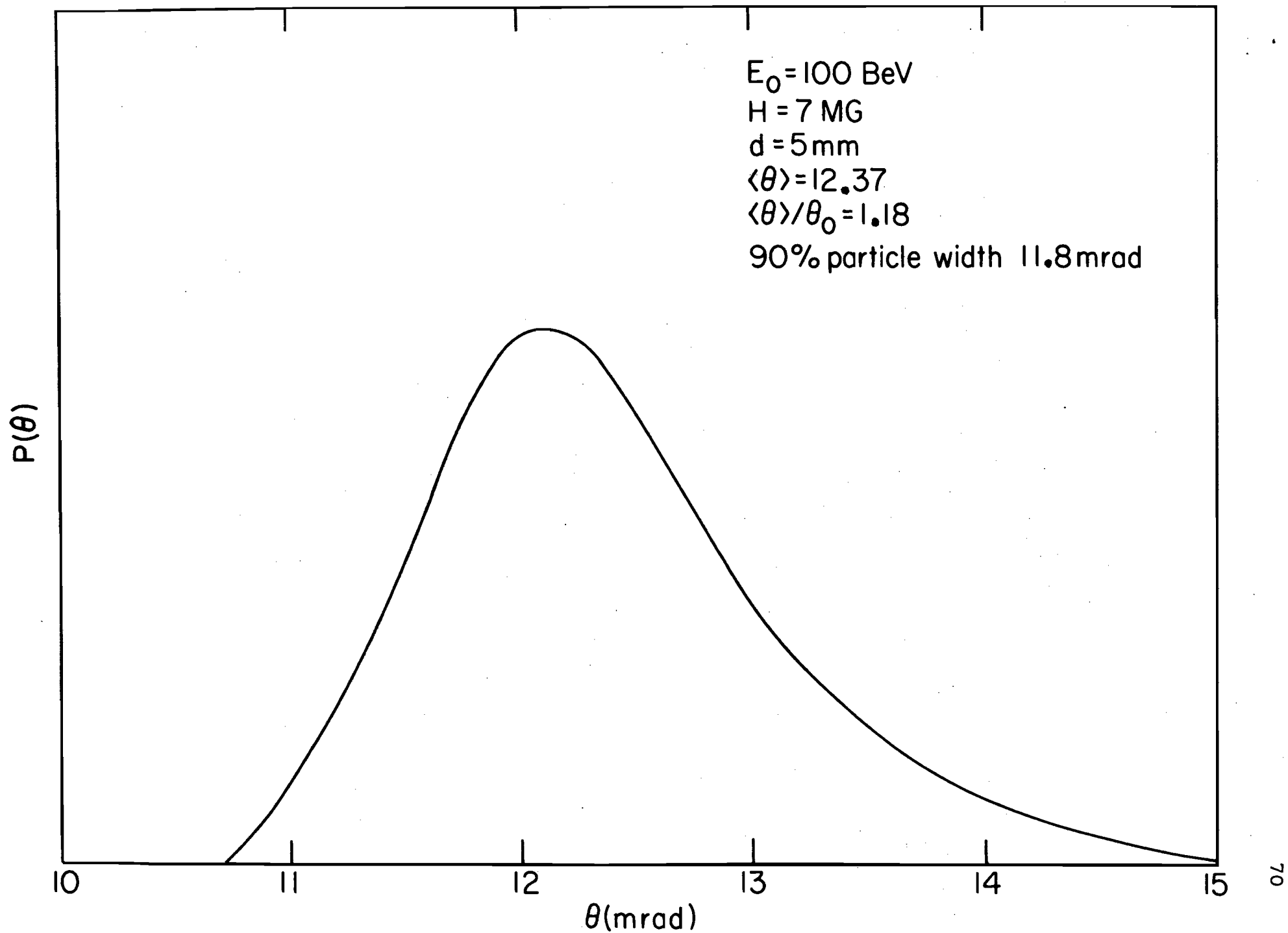


Fig. 4

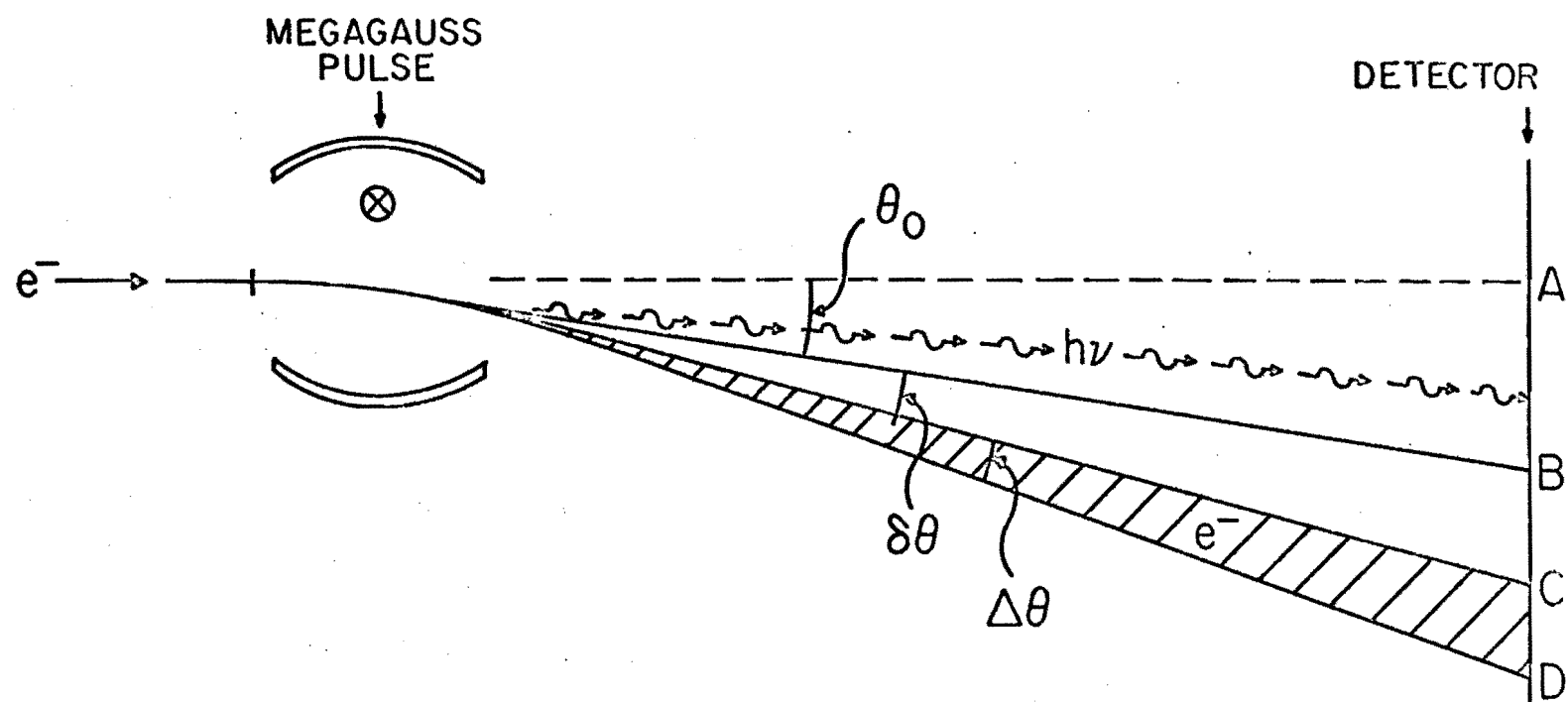


Fig. 5



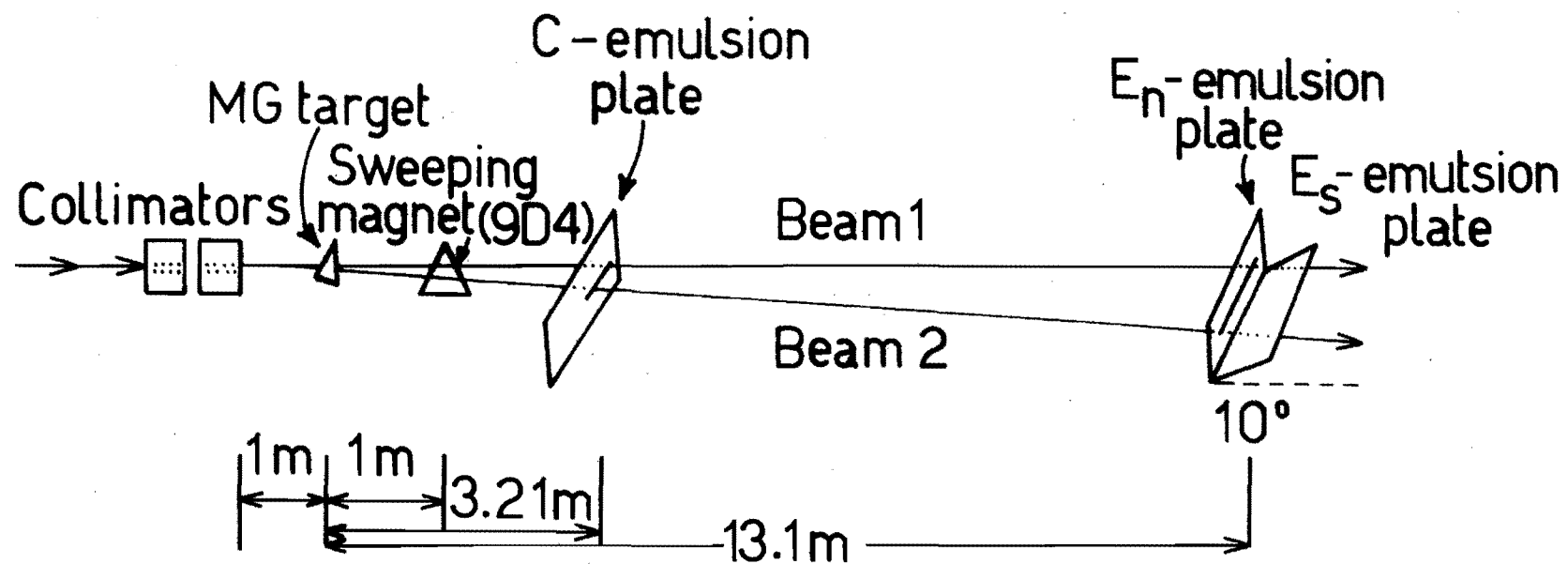
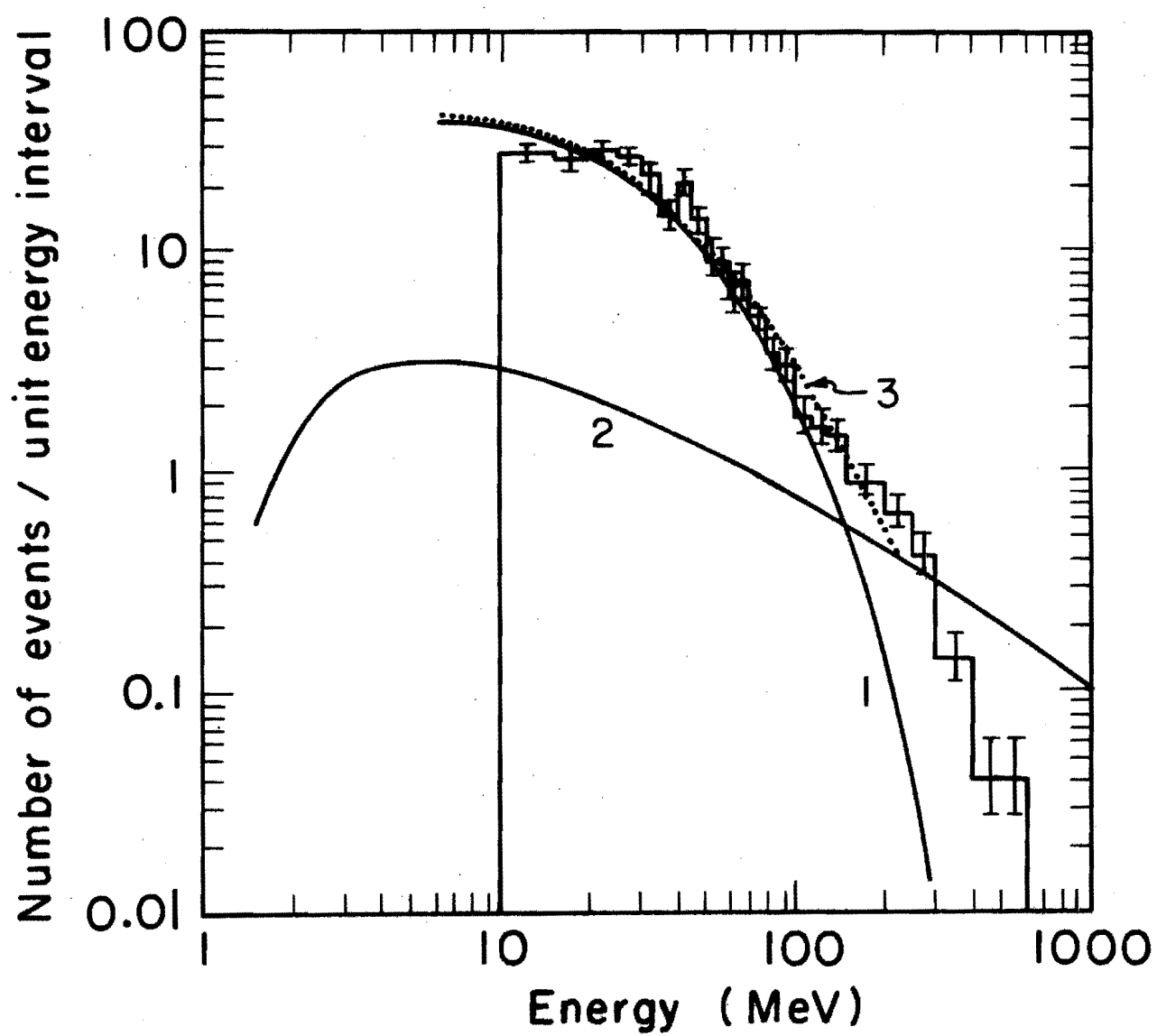


Fig. 6



XBL725-2871

Fig. 7

## 9(a). Budget - IIT Portion

[1 June 1973 - 1 June 1975]

		<u>First Year</u>	<u>Second Year</u>
1.	<u>Salaries</u>		
Dr. T. Erber, Professor	Academic year [2 semesters; 25%] Summer [2 months]	5,100 4,266	5,400 4,522
Dr. H. G. Latal, Senior Research Associate	4 months [100%]		4,800
Dr. D. White Research Associate	12 months [100%]	11,500	12,000
Dr. K. Abe, Research Associate	12 months [100%]	11,500	12,000
R. Olenick, Graduate Assistant	Academic year and summer	5,500	5,700
Technician	Full time	10,500	10,700
Secretary	Half time	3,000	3,000
Technical Assistance		2,200	2,200
Employee Benefits (5% of salaries)		2,678	3,016
2.	<u>Non-Expendable Equipment</u>		
Capacitors [30 Sangamo #740515]		10,800	
Bran-Rex cable [2500 ft. of V-1633]		4,400	
Tektronix oscilloscopes - repair and align 9 type 556		1,100	
Bank termination and collector plate		3,800	
Safety shield, venting system, stabilized power (30 kW)		12,000	
Shielded room (Lindgren #34)		4,000	
Thyratron pulser			6,000
Pulse transformers (2)			450
Flash X-ray channel [F.E. 1563/1027]			4,840

	<u>First Year</u>	<u>Second Year</u>
Digital delay generator [Cordin 432]		5,600
Plate Holders [2 NCR 800]		550
Ball screw feed for Bridgeport mill base		2,100
Mill base, NC channels, motors & boosters, swing plate for MG-target		18,000
3. <u>Expendable Equipment</u>		
Coil assemblies	1,500	1,500
Dielectric switch components	1,100	800
Test jigs and MG-sensors	600	600
Film, emulsions	600	800
Miscellaneous electronics	2,000	2,000
4. Travel (Purdue-IIT-NAL)	500	500
Travel (Meetings)	600	600
Travel (Graz-IIT-Graz)		600
Shipping costs for equipment (IIT-NAL)		850
5. Computer time, service contract on HP-9100	1,750	1,750
6. Publication costs	1,500	1,500
7. Indirect costs (50% of salaries)	28,122	31,669
8. Research at Purdue (see p. 76)	24,169	24,981

## 9(b) Budget - Purdue Portion

[1 June 1973 - 1 June 1975]

	<u>First Year</u>	<u>Second Year</u>
1. <u>Salaries</u>		
Dr. C. S. Shen, Professor		
Academic year (2 semesters; 25%)	4,550	4,800
Summer (2 months)	3,640	3,840
One Graduate Student FY 75%	3,960	3,960
Employee Benefits (11.6% of salaries)	1,407	1,479
2. Travel (IIT-NAL)	300	300
Travel (Meetings)	400	400
3. Computer	600	600
4. Publication	1,500	1,500
5. Indirect costs (64.3% of Salaries)	7,812	8,102
<u>Summary</u>		
Salaries	13,557	14,079
Travel and Shipping	700	700
Computation	600	600
Publication costs	1,500	1,500
Indirect costs	<u>7,812</u>	<u>8,102</u>
	\$24,169	\$24,981

## 9 (c) Total Budget

Summary

Salaries	56,244	63,338
Non-expendable Equipment	36,100	37,540
Expendable Equipment	5,800	5,700
Travel and Shipping	1,100	2,550
Computation	1,750	1,750
Publication Costs	1,500	1,500
Indirect Costs	28,122	31,669
Research at Purdue	<u>24,169</u>	<u>24,981</u>
	\$154,785	\$169,028

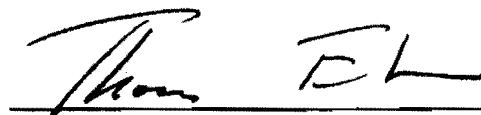
## 10. Sponsorship

This proposal is being submitted to the Atomic Energy Commission and the National Science Foundation.

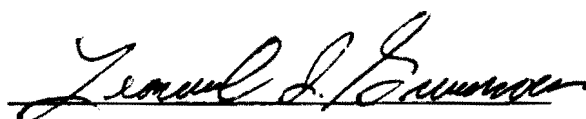
Preliminary discussions concerning the Bremsstrahlung experiments have already been held with NAL. A plan for the experiment is concurrently being submitted to NAL for technical approval and inclusion in their research schedule.

The activities of the IIT Magnet Laboratory are currently supported by NSF Grants GH-34664, GP-12338; and the Research Corporation. Professor Shen's work at Purdue is supported by a grant from the Purdue Research Foundation

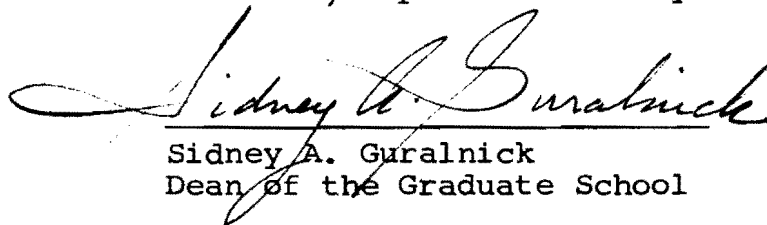
Illinois Institute of Technology will be pleased to undertake the outlined program, to discuss any modifications, and to administer a research grant awarded in accordance with the foregoing proposal.



Thomas Erber  
Principal Investigator

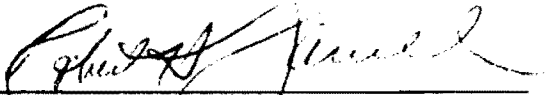


Leonard I. Grossweiner  
Chairman, Department of Physics



Sidney A. Guralnick  
Dean of the Graduate School

I certify that the distribution of costs between the direct and indirect categories as shown in the proposal conforms to the usual accounting practices of the Institution and to the distribution used by the cognizant Federal audit agency.

  
\_\_\_\_\_  
Robert H. Jarrell  
Business Manager

Nov. 22, 1972  
\_\_\_\_\_  
Date



# 11. Proposed Layout of Megagauss Facility at NAL

- (a) Location: Behind experiment #25A in the A-beam line of the Proton Laboratory.

The choice of distance between experiment #25A and the megagauss area should satisfy the following criteria:

- (1) Adequate radiation safety [allowance of sufficient space for beam dumps, stoppers, and shielding].
- (2) Protection of instrumentation associated with #25A against EMI from high energy capacitor bank discharges.
- (3) Adequate beam length for the insertion of collimation, focusing, and beam sweep elements.
- (4) Attenuation of ground shocks from explosive charges in helical generators [Phase IV].
- (5) Reasonable cost of beam installation.

(1), (2), and (4) lead to lower limits of the order of 100'. Strictly speaking, (3) refers to the minimum length of beam line required upstream from the megagauss targets; conceivably some elements of this beam line could be interspersed with the components associated with #25A, or even be located upstream from #25A. However, as emphasized in Section 7, experience at SLAC showed that this kind of multiplexing could actually decrease flexibility in beam switching and become the major factor in boosting demands for accelerator time. For this reason we strongly recommend that most of the elements of the A-Bremsstrahlung beam be located downstream from the #25A area [see Fig. 8]. The most critical lower bound on the distances associated with the beam optics is set by the geometry of the pulsed magnet that chops the beam down to a

0.1  $\mu$ sec burst [compare Table 1 and Section 7]. If we assume beam sweep velocities of the order of 1 mm/0.1  $\mu$ sec, and pulsed power supply ["hard tube" pulser] ratings of 5 kA at 7 kV, then the minimum distance between the pulsed magnet that shutters the beam and the last collimator must be at least 300'.

(b) Size of Experimental Area: The space requirements will be approximately equivalent to those of the SLAC set-up [see appended blue print].

(1) Main Experimental Area - this will contain the target, bank, and detector modules (see p. 60). The minimum (or third preference) requirement is an area 16' wide x 40' long, with concrete pads to support the mill bases and the condenser bank. Our second preference is 20' wide x 40' long with concrete flooring throughout. Our first preference is 20' wide x 100' long, concrete flooring throughout---the added length would accommodate the counting equipment required for phase II (p. 7). Removeable roof sections, access for cranes, or other means entry must be provided for delivery of heavy equipment, e.g. mill bases and bank modules. Provision must be made to keep the humidity in this area at low levels. Experience at SLAC showed that even a slight amount of sweating could cause dangerous arc-overs on the condenser bank.

(2) RF Shielded Room - 12' x 12' room with (electrically shielded) 28,000 BTU (minimum rating) air conditioner. This room should be located not more than 50' from the MG-target. It should be protected from the weather, particularly the extra heat load of the summer sun; and be conveniently accessible from the main experimental area as well as the control room [compare (3b) on p. 60].

---

(3) Control Room/Work Area - 12' x 50' all weather enclosure housing all control circuits (p. 60); laboratory equipment required for dielectric switch replacement, and general, test, and servicing; experimenters' office space.

Areas (1), (2), and (3) should be linked by cable trays and intercom circuits. A tentative layout is shown on Fig. 9.

(c) Utilities:

(1) Electricity - 40 kVA (220/110 AC), normal regulation, for all instrumentation, power supplies, air conditioners, and dehumidifiers. This estimate does not include power for illumination.

(2) Water - cold water will probably be required for cooling some of the collimators in the beam line, as well as the radar tubes in the pulsed magnet power supplies.

(3) Communications - telephone extensions in main experimental area and control room; intercom linking main experimental area-control room-shielded room; intercom linking control room to accelerator control.

(d) Safety Requirements

(1) Radiation - interlocks with beam stoppers downstream from #25A experiment; controlled access (2 doors--see Fig. 9) to main experimental area when beam is brought to MG target.

(2) High Energy Condenser Bank - conventional high voltage wiring techniques for all hazardous components; protection of bank module against capacitor rupture; manually operated fire extinguishers [at SLAC a remotely controlled, rapid acting, fire extinguishing

system was installed]; interlocks with controlled access doors.

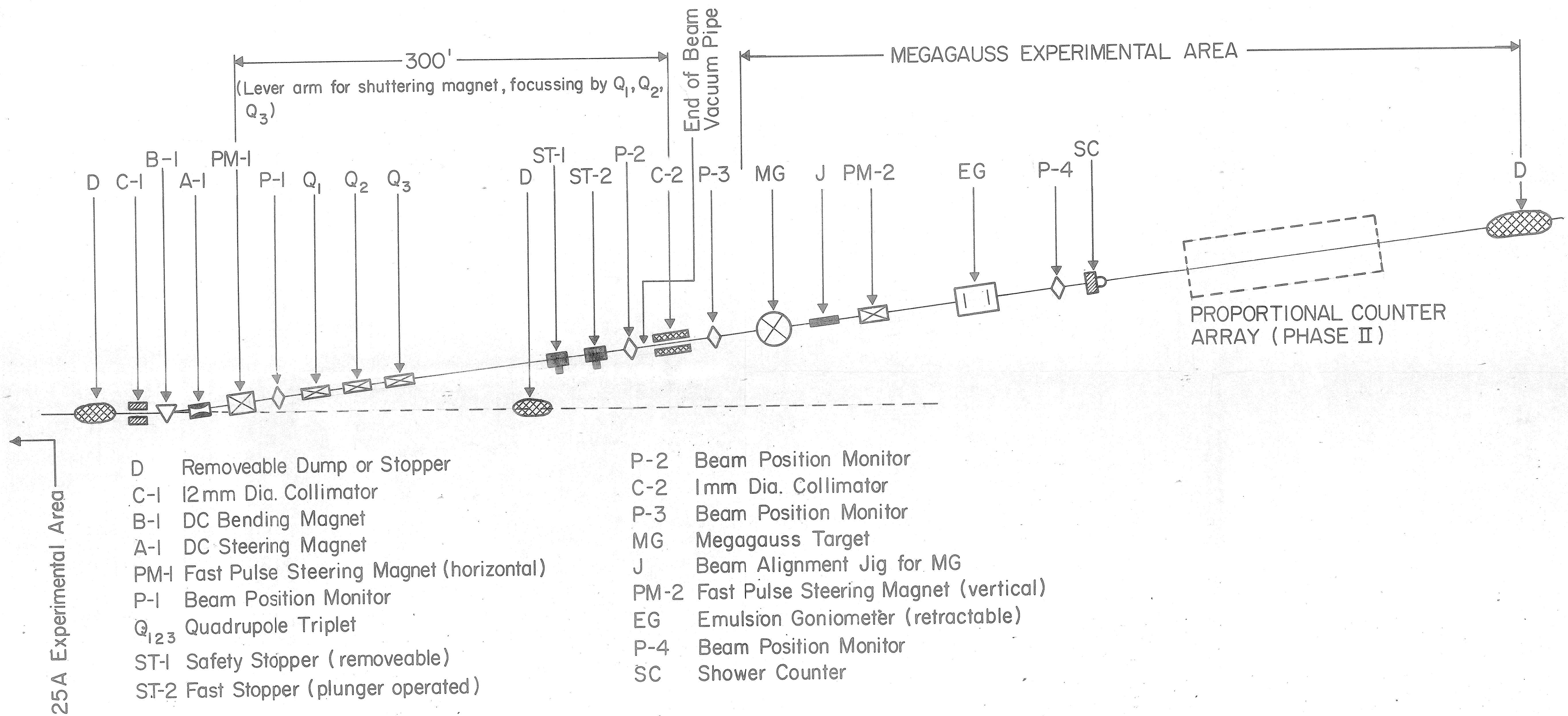
[Compare AEC "Serious Accident" No. 287, April 1968.]

(3) Electrical Surges and Noise - interlocked bank charging supplies; installation of special grounding bus lines.

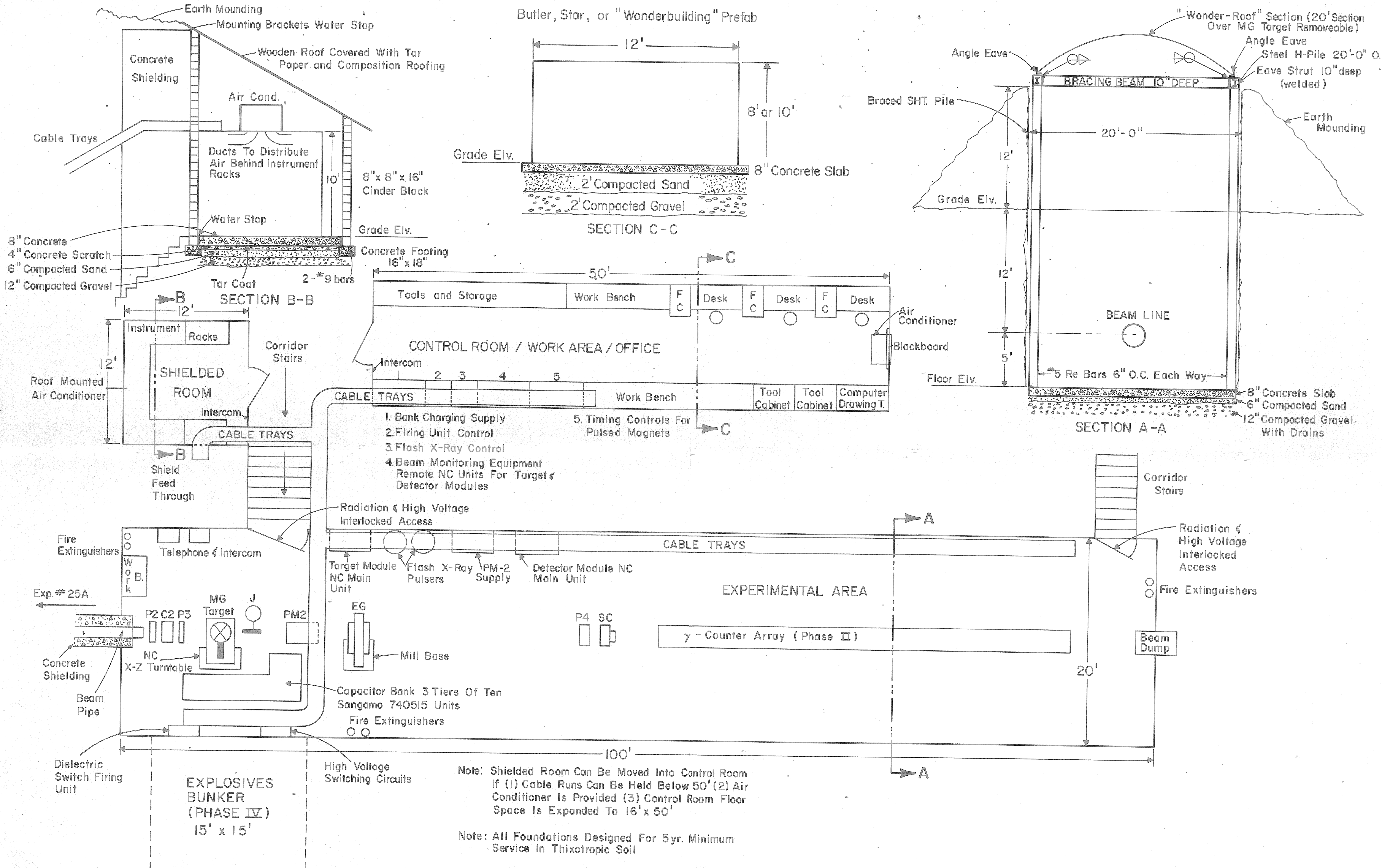
(4) Megagauss Targets - mechanical shielding provided to prevent shrapnel damage to instruments and beam line.

(5) Helical Generators (Phase IV) - special bunker (Fig. 9); storage of all high explosive components at IIT Magnet Laboratory, KOP site; observance of all safety regulations applicable to transporting, handling, and installing high explosive components.

(e) Construction of Megagauss Facility: The IIT Magnet Laboratory is prepared to furnish extensive assistance with the design and construction of the megagauss area at NAL. We have access to engineers and contractors who are experienced in the erection of specialized laboratory facilities. This team was responsible for the construction of the explosives complex of the IIT Magnet Laboratory at KOP.

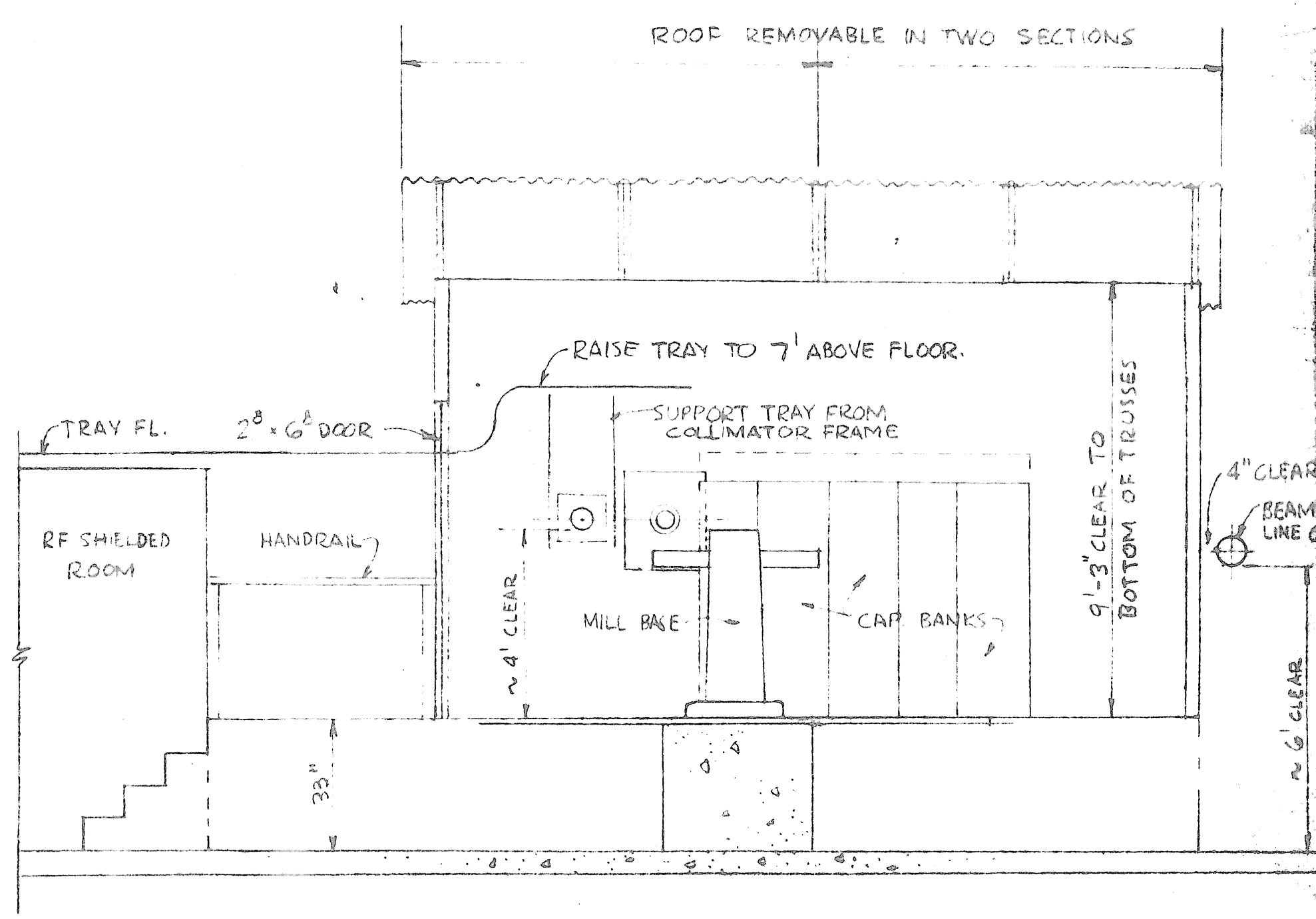
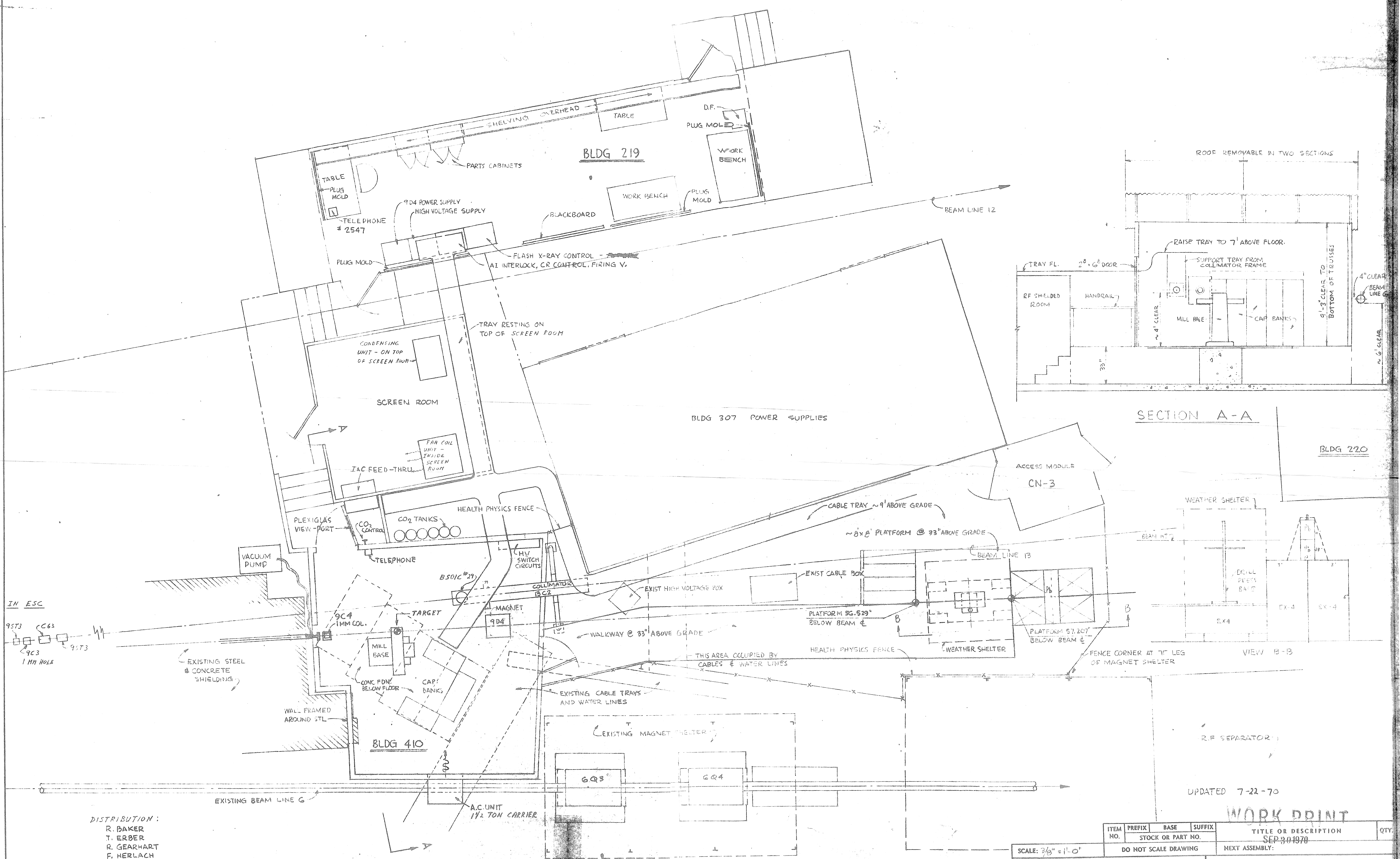




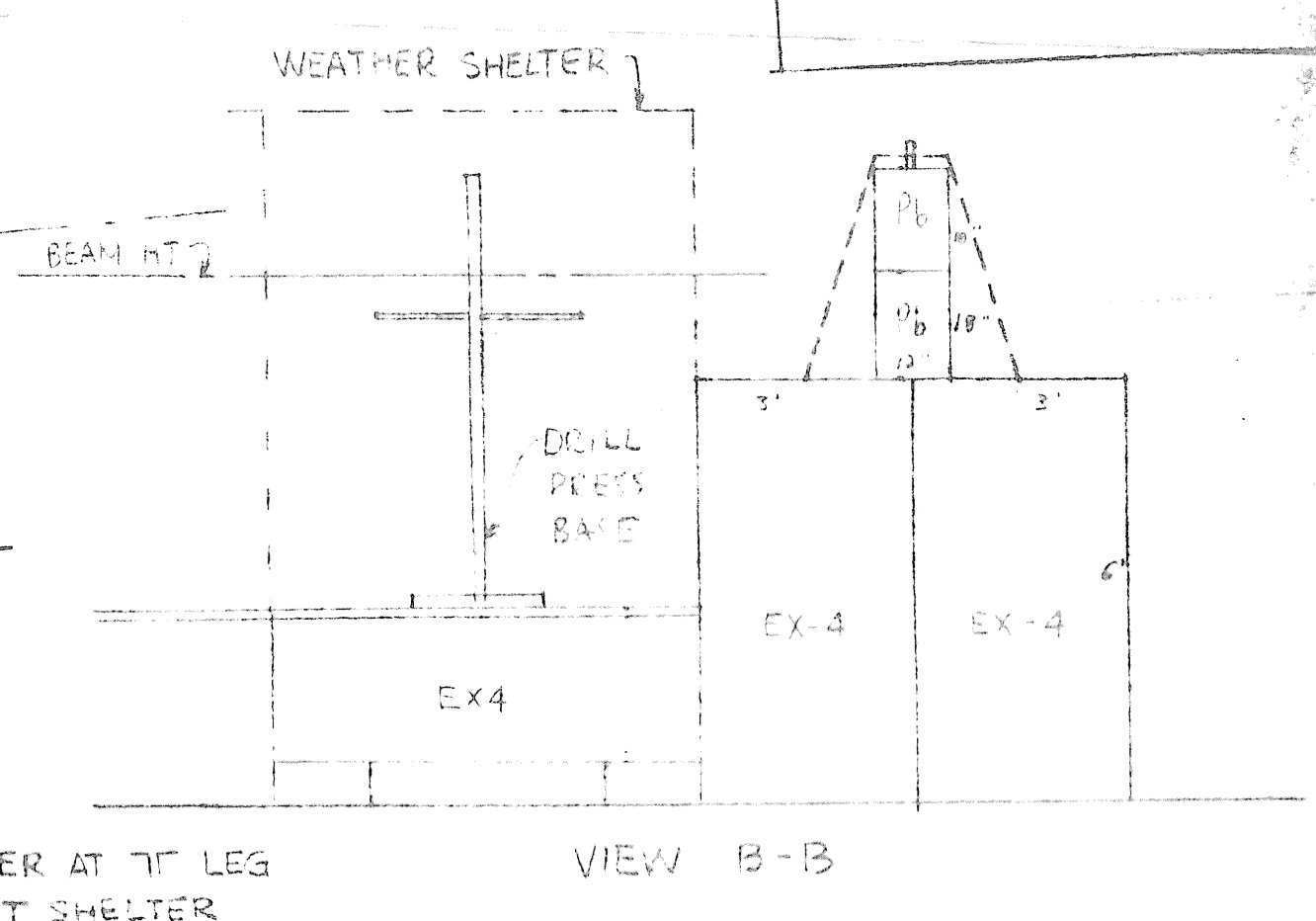




REV.	DESCRIPTION	DRN	CHK	APP
------	-------------	-----	-----	-----



SECTION A-A



VIEW B-B

DISTRIBUTION:  
R. BAKER  
T. ERBER  
R. GEARHART  
F. HERLACH  
E.K. JOHNSON  
E. KEYSER

PLOT PLAN

SCALE: 3/8" = 1'-0"				ITEM NO.		PREFIX		BASE		SUFFIX		TITLE OR DESCRIPTION		QTY.	
STANFORD LINEAR ACCELERATOR CENTER				DO NOT SCALE DRAWING		STOCK OR PART NO.		NEXT ASSEMBLY:		EXPERIMENT D-9		CENTRAL BEAM		PLOT PLAN	
U.S. ATOMIC ENERGY COMMISSION				STANFORD UNIVERSITY		STANFORD, CALIFORNIA		DATE		APPROVALS		GP 405-118-00		RO F	
PROPRIETARY DATA OF STANFORD UNIVERSITY AND/OR U.S. ATOMIC ENERGY COMMISSION. RECIPIENT SHALL NOT PUBLISH THE WITHIN INFORMATION WITHOUT SPECIFIC PERMISSION OF STANFORD UNIVERSITY.				ENGINEER: E.T. HALBO		DATE: 7-22-70		CHECKED: E.T. HALBO		APPROVED: E.T. HALBO		GP 405-118-00		RO F	